

# RSC Advances



This is an *Accepted Manuscript*, which has been through the Royal Society of Chemistry peer review process and has been accepted for publication.

*Accepted Manuscripts* are published online shortly after acceptance, before technical editing, formatting and proof reading. Using this free service, authors can make their results available to the community, in citable form, before we publish the edited article. This *Accepted Manuscript* will be replaced by the edited, formatted and paginated article as soon as this is available.

You can find more information about *Accepted Manuscripts* in the [Information for Authors](#).

Please note that technical editing may introduce minor changes to the text and/or graphics, which may alter content. The journal's standard [Terms & Conditions](#) and the [Ethical guidelines](#) still apply. In no event shall the Royal Society of Chemistry be held responsible for any errors or omissions in this *Accepted Manuscript* or any consequences arising from the use of any information it contains.

## A Novel Benzimidazole Derivative Binds to DNA Minor Groove and Induces Apoptosis in Leukemic Cells

Mahesh Hegde<sup>a</sup>, Kothanahally S. Sharath Kumar<sup>a</sup>, Elizabeth Thomas<sup>b</sup>, Ananda Hanumappa<sup>a</sup>, Sathees C. Raghavan<sup>b\*</sup> and Kanchugarakoppal S. Rangappa<sup>a\*</sup>

<sup>a</sup>Department of Studies in Chemistry, Manasagangotri, University of Mysore, Mysuru-570006; <sup>b</sup> Department of Biochemistry, Indian Institute of Science, Bangalore-560012.

Running title: Identification of a novel DNA minor groove binder.

Key words: Double-strand break, Apoptosis, Chemotherapy, DNA binder, Minor groove, Genomic instability, Topoisomerase

\*Corresponding author

Kanchugarakoppal S. Rangappa      Ph.: +91-821-2419661; Fax: +91-821-2500846  
e-mail: [rangappaks@chemistry.uni-mysore.ac.in](mailto:rangappaks@chemistry.uni-mysore.ac.in)

Sathees C. Raghavan                      Ph.: +91 80 2293 2674; Fax: 091 80 2360 0814  
e-mail: [sathees@biochem.iisc.ernet.in](mailto:sathees@biochem.iisc.ernet.in)

## Abstract

DNA minor groove binder is an important class of chemotherapeutic agents. These small molecule inhibitors interfere with various cellular processes like DNA replication and transcription. Several benzimidazole derivatives showed affinity towards DNA minor groove. In this study we show the synthesis and biological studies of novel benzimidazole derivative (**MH1**), that inhibits topoisomerase II activity and *in vitro* transcription. UV-visible and fluorescence spectroscopic methods in conjunction with Hoechst displacement assay demonstrate that **MH1** binds to DNA at the minor groove. Cytotoxic studies showed that leukemic cells are more sensitive to **MH1** compared to cancer cells of epithelial origin. Further, we find that **MH1** treatment lead to cell cycle arrest at G2/M, at early time points in Molt4 cells. Finally multiple cellular assays demonstrate that **MH1** treatment leads to reduction in MMP, induction of apoptosis by activating CASPASE 9 and CASPASE 3. Thus our study shows **MH1**, a novel DNA minor groove binder, induces cytotoxicity efficiently in leukemic cells by activating intrinsic pathway of apoptosis.

## INTRODUCTION

Targeting DNA, the genetic material of a cell, is considered as one of the most attractive chemotherapeutic targets and DNA interacting compounds are known to inhibit growth of cancer cells <sup>1</sup>. Since growth rate of cancer cells is high, it serves as an important strategy to target DNA molecules in order to interrupt replication, which is essential in each cell division of the cancer cell <sup>2</sup>. Grooves in DNA are associated with several biological interactions inside the cell. The major groove which is wide and approximately 24 Å in width helps in majority of protein DNA interactions, whereas the narrow minor groove which is only 10 Å in width, is an attractive target for small molecular inhibitors <sup>3</sup>.

Reversible interactions of small molecules with DNA have been majorly classified into three subgroups; intercalation, groove binding and electrostatic interactions <sup>4</sup>. Studies on the minor groove of DNA interaction with noncovalent small molecules has resulted in emerging of many small molecule inhibitors as anticancer agents <sup>5</sup>. Many natural products have also shown significant interactions with DNA minor groove <sup>6</sup>. DNA interacting agents majorly affect replication and transcription activities inside the cell <sup>7</sup>. Importantly, DNA minor groove binders are found to inhibit the topoisomerase activity and subsequent cell cycle arrest <sup>8</sup>.

Benzimidazole moiety is structurally related to purine bases and is found in a variety of natural products, such as vitamin B12. Benzimidazole nucleus is termed “master key” as it is an important core in many bioactive compounds. Different benzimidazole derivatives act at various targets within the cells to elicit an array of pharmacological properties <sup>9</sup>. It is one of the most extensively studied class of heterocyclic compounds with wide range of biological activities such as anti-HIV <sup>10</sup>, antioxidant <sup>11</sup>, antifungal <sup>12</sup>, antiviral <sup>13</sup>, antibacterial <sup>14</sup>, antimycobacterial <sup>15</sup> and they are well known to possess antitumor/anticancer activity <sup>16</sup>. Importantly, benzimidazole derivatives were found to interact with DNA <sup>17</sup> and were also used in the medicinal field where the primary target was found to be DNA and DNA associated processes <sup>18</sup>.

In the present study, we have designed and synthesized novel 2,5 di and 2,5,7 tri substituted benzimidazole derivatives as shown in scheme 1 and scheme 2 (**Figure 1 and 2**), and evaluated their anticancer activity against various cancer cell lines. **MH1** was identified as the most potent small molecule inhibitor. **MH1** exhibited DNA binding properties as determined by various biophysical assays, and inhibited both topoisomerase and transcription reactions. Further, *ex vivo* studies showed that novel benzimidazole derivative, **MH1** treatment led to decrease in mitochondrial membrane potential and induced intrinsic pathway of apoptosis resulting in cytotoxicity in leukemic cells.

## RESULTS

### Synthesis of novel benzimidazole derivatives

The general approach for the synthesis of 2,5-disubstituted (**MH1** and **2**) and 2,5,7-trisubstituted benzimidazoles (**MH3-5**) is outlined in scheme-1 and scheme-2, respectively (**Figure 1 and 2**). As depicted in the schemes, different aryl substitution on C-5 and C-7 of benzimidazole backbone has been achieved by using an appropriate phenyl boronic acid. Thus, for the first time we describe direct tri aryl substitution on C-2, C-5 and C-7 positions of benzimidazole ring.

We have synthesized compounds **MH1** and **MH2** as shown in scheme-1. Nitro group reduction of 4-Bromo-2-nitroaniline (**1**) with commercial zinc dust along with catalytic amount of HCl in ethanol under reflux condition obtained 4-Bromo-1,2-diaminobenzene (**2**).

In continuation to our previous efforts <sup>19</sup> we constructed benzimidazole ring using T3P® as a cyclodehydrating agent. T3P® mediated cyclocondensation of 4-bromo-1,2-diaminobenzene (**2**) with p-Tolualdehyde in ethylacetate produced compound **3** with excellent yield. The substitution of aryl group at C-5 and C-7 of benzimidazole ring was effected with a Suzuki coupling protocol in both scheme 1 and scheme 2. Para alkyl substituted aryl boronic acids were used to make C-C bond using

Bis(triphenylphosphine)palladium(II) dichloride as a catalyst and potassium carbonate as a base under Suzuki reaction condition to obtain the title compounds, **MH1-5**.

### **MH1 effectively inhibits the proliferation of leukemic cells**

Cytotoxic effect of newly synthesised benzimidazole derivatives were tested on different cancer cell lines using MTT assay. Results showed that among the five benzimidazole derivatives studied, **MH1** showed maximum cytotoxicity in all the tested cell lines (**Figure 3A**). **MH1** exhibited an IC<sub>50</sub> of 5.5, 8.9, 13.83 and 13.3  $\mu\text{M}$  in leukemic cell lines, Molt4, Nalm6, REH and K562, respectively. However, **MH1** was less effective, when tested in MCF7, HeLa and EAC cells, compared to leukemic cells (**Figure 3A**). Hence our results suggest that leukemic cells are more sensitive to **MH1** compared to cancers of epithelial origin. Sensitivity of **MH1** was further evaluated at varying concentrations (0-20  $\mu\text{M}$ ), for 48 and 72 h in Molt4, Nalm6, REH and K562 cells. Highest concentration of DMSO treated cells served as vehicle control for the study. Results showed that among the leukemic cells tested, Molt4 exhibited maximum sensitivity to **MH1**, both in a dose and time dependent manner (**Figure 3B**). Thus, Molt4 was selected for further studies.

### **MH1 induces G2/M arrest and results in accumulation of SubG1 cells**

Based on the above results, we wondered whether **MH1** treatment could induce cell cycle arrest in Molt4 and K562 cells. In order to test this, Molt4 and K562 cells were treated with increasing concentrations of **MH1** (1, 5, 10 and 20  $\mu\text{M}$  for 48 h). PI staining followed by flow cytometry analysis, revealed a concentration dependent accumulation of SubG1 phase cells in both Molt4 and K562 cells (**Figure 4A, B, C and D**). Interestingly, we also observed a G2/M arrest at a lesser extent in both the cell lines tested, particularly at 5-10  $\mu\text{M}$  (**Figure 4B and D**).

Interestingly the treatment of **MH1** (10  $\mu\text{M}$ ) in Molt4 cells showed a prominent cell cycle arrest at G2/M phase at both 6 and 12 h time points (**Figure 4E and F**). Thus our data

suggests that **MH1** could induce G2/M arrest at initial time points and increase SubG1 phase cell population at later time points, thereby inhibiting the proliferation of leukemic cells.

### **Apoptosis is induced in MH1 treated cells**

Mode of cell death following **MH1** treatment was analysed in Molt4 cells using Annexin-FITC/PI staining. Movement of phosphatidylserine from inner membrane surface to outer membrane surface following cellular damage is an indicator of apoptosis, and can be studied following double-staining with Annexin-FITC and propidium iodide (PI). Treatment of increasing concentrations of **MH1** (48 h) resulted in significant increase in early and late apoptotic cells (**Figure 5A**). Necrotic cells were either absent or minimal after treatment with **MH1** (**Figure 5B**). Besides, confocal microscopic analysis confirmed the staining of Annexin-FITC alone or both Annexin-FITC and propidium iodide staining in **MH1** treated Molt4 cells (**Figure 5C**). Thus, **MH1** treatment showed activation of apoptosis in Molt4 cells.

### **Assessing the effect of MH1 on Molt4 cells using calcein-AM and ethidium homodimer staining**

Calcein-AM and ethidium homodimer staining was used to analyse both live and dead cells, respectively in Molt4 cells following treatment with increasing concentrations of **MH1** (0, 1, 5 and 10  $\mu$ M for 48 h) (**Figure 6A**). Results showed increase in cells stained with both calcein-AM and ethidium homodimer upon treatment with **MH1** in concentration dependent manner (**Figure 6A and B**). These results further confirm the cell death following treatment with **MH1**.

### **DNA fragmentation assay**

DNA ladder formation is the hallmark of cellular apoptosis<sup>20</sup>. **MH1** treated Molt4 cells showed prominent DNA fragmentation at 48 h time point in a concentration dependent manner (**Figure 6C**). Compared to the DMSO treated vehicle control cells, **MH1** treated cells

showed ladder formation from 5  $\mu\text{M}$  onwards in a concentration dependent manner (**Figure 6C and D**).

### **MH1 treatment lead to reduction in mitochondrial membrane potential**

To check the effect of **MH1** on mitochondrial membrane potential (MMP), JC-1 staining was performed. Interestingly, **MH1** treated (0, 1, 5, 10 and 20  $\mu\text{M}$ ) Molt4 cells showed significant reduction in MMP in a concentration dependent manner. There were three different population of cells with altered MMP observed, having high, intermediate and low MMP. Following **MH1** treatment, we observed a prominent shift of high MMP cells to intermediate or low MMP in a concentration dependent manner (**Figure 7A and B**). Thus, our results suggest that apoptosis induced by **MH1** on Molt4 cells could be due to mitochondrial apoptotic pathway.

### **MH1 induces apoptosis through intrinsic pathway**

Based on promising results observed from JC-1 staining assay we carried out western blotting analysis for expression of apoptotic markers. Molt4 cells treated with different concentration of **MH1** were subjected to immunoblotting analysis. Interestingly, we observed an up regulation of BAX expression, a protein involved in mitochondrial mediated apoptosis, following **MH1** treatment (**Figure 7C**). BCL2, an anti-apoptotic protein showed no significant difference in the expression in control and treated cases. However, distinct bands due to cleavage of both CASPASE9 and CASPASE3 were observed (**Figure 7C and D**) following treatment with **MH1**. Hence, immunoblotting results suggest that **MH1** treatment resulted in activation of intrinsic pathway of apoptosis in Molt4 cells <sup>21</sup>.

### **MH1 binds to minor groove of DNA**

To test whether **MH1** binds directly to DNA, UV-visible and fluorescence emission spectroscopic studies were carried out in presence of calf thymus (CT) DNA <sup>22</sup>. UV-visible



spectroscopy showed two characteristic absorption peaks for **MH1** at 259 and 315 nm. Upon serial increase in the concentrations of CT-DNA, a characteristic decrease in the absorption at both 259 and 315 nm was observed, which can be directly correlated to the ability of **MH1** to intercalate DNA or bind to groove of DNA (**Figure 8A**).

To confirm the binding interaction of **MH1** with DNA, we took the advantage of fluorescent properties of **MH1**<sup>23</sup>. **MH1** exhibited a fluorescent excitation (259 nm) and emission maxima (315 nm and 385 nm). Interestingly, we observed that the fluorescence emission spectra of **MH1** was decreased when incubated with increasing concentrations (0, 1, 5, 10, 25, 50, 75 and 100  $\mu$ M) of CT-DNA, which confirmed above observation of binding of **MH1** to DNA (**Figure 8B**).

In order to test the mode of **MH1** and DNA interaction, we performed DNA dye displacement assay, a test used for differentiating the intercalators and minor groove binders<sup>24</sup>. We find that addition of **MH1** (0, 1, 5, 10, 25, 50 and 100  $\mu$ M) to Hoechst 33258-DNA complex decreased the characteristic emission spectra of Hoechst in a concentration dependent manner (**Figure 8D**). However, **MH3**, a less potent compound with extra benzene ring at the seventh position on benzimidazole ring, did not induce significant change in emission spectrum (**Figure 8D**), which suggested plausible **MH1** interactions with minor groove of the DNA. It is possible that unlike **MH1**, the extra benzene ring at the seventh position on benzimidazole ring may cause a hindrance for binding to DNA. Besides, ethidium bromide dye displacement assay was also performed to check the intercalating properties of **MH1**. Interestingly, addition of **MH1** did not change the emission spectra of ethidium bromide along with DNA confirming the observation that **MH1** is not a DNA intercalator (**Figure 8C**). However, there was a marginal topological alteration, when CT-DNA was added to **MH1** and analysed using circular dichroism studies (**Figure 9**).

**MH1 interferes with some of the DNA protein transactions**

Previous studies have shown that small molecules that bind DNA minor groove can affect topoisomerase action <sup>25</sup>. We tested whether **MH1** could interfere with human topoisomerase I and II. To test this supercoiled plasmid DNA (250 ng) was incubated with topoisomerases in presence of increasing concentrations of **MH1** (10, 25, 50 and 100  $\mu$ M) and the products were resolved on an agarose gel. Results showed that **MH1** inhibited topoisomerase II $\alpha$  mediated conversion of supercoiled DNA to circular form in a concentration dependent manner (**Figure 9A**). Etoposide (100  $\mu$ M) was used as the positive control. However, such an effect by **MH1** was absent or minimal when topoisomerase I was used for the study (**Figure 9B**).

We tested whether DNA binding ability of **MH1** could result in inhibition of other cellular processes like transcription. Inhibitory effect of **MH1** on *in vitro* transcription on a plasmid DNA by T7 polymerase was tested and the reaction products were visualized on an agarose gel. Addition of **MH1** (10, 25, 50 and 100  $\mu$ M) inhibited formation of RNA species during transcription in a concentration dependent manner (**Figure 9C**). Hence our results indicate that DNA groove binding by **MH1** could interfere with cellular processes drastically <sup>26</sup>, thereby causing cell cycle arrest and apoptosis in cancer cells.

In order to have further insight on **MH1** interaction with the minor groove of DNA, docking studies were carried out. Results suggested that **MH1** can efficiently occupy the minor groove of DNA (Hoechst 33258 binding site) with a binding energy of -9.84 kcal/mol (**Figure 10A, B**). Hydrogen bond Interactions of hydroxyl group of thymine and imidazole moiety of **MH1** favoured the affinity of **MH1** towards the DNA (**Figure 10C**). Thus spectroscopic studies in conjunction with docking results suggested that **MH1** binds to minor groove of DNA.

## DISCUSSION

In the current study, we have developed a facile, direct and efficient method for the synthesis of highly substituted benzimidazole derivatives. The present method is efficient for the chemo selective synthesis of various 2,5,7 tri aryl substituted benzimidazole derivatives.

Cytotoxicity results of newly synthesized compounds on different cancer cell lines showed prominent or moderate cytotoxicity, among all synthesized compounds. Among the molecules studied, **MH1** was most promising molecule with notable IC<sub>50</sub> values in all cancer cell lines tested (**Figure 3A**). Interestingly, effect of **MH1** was more pronounced in leukemic cell lines, especially, Molt4 cells showed highest sensitivity among all tested cell lines (**Figure 3B**).

The overall structure of **MH1** and **MH2** is in a crescent shape which is characteristic of typical minor groove binding ligands. In addition the nitrogen atom in the benzimidazole core has the ability to form a hydrogen bond with nucleotides. Besides, these molecules possess sufficient conformational flexibility to further help in attaining the shape, which is significant enough to fit inside the DNA minor groove<sup>17</sup>. As observed in the cytotoxicity assays (**Figure 3B**), cancer cell lines showed higher sensitivity towards **MH1** and **MH2**, compared to rest of the compounds, which possess an extra benzene ring. It appears that the extra benzene ring could diminish the solubility of the compound as well as binding to the DNA minor groove. This explains the reduced cytotoxicity exhibited by **MH3-5** as compared to **MH1-2**.

**MH1** treatment on Molt4 cells at 6 and 12 h resulted in G2/M arrest while at 48 h time point resulted in accumulation of SubG1 phase cells in a concentration dependent manner (**Figure 4**). Further, Annexin-FITC/PI staining of **MH1** treated Molt4 cells showed induction of apoptosis both by flow cytometry and confocal microscopy (**Figure 5**). Live dead assay using calcein-AM and ethidium homodimer staining corroborated the above findings (**Figure 6**). DNA ladder formation in **MH1** treated Molt4 cells further confirmed induction of apoptosis (**Figure 6C and D**).

Interestingly, **MH1** treatment resulted in lowering of mitochondrial membrane potential in Molt4 cells (**Figure 7A and B**). Western blotting assays for apoptotic markers confirmed the involvement of mitochondrial machinery in activating intrinsic pathway of apoptosis (**Figure 7C and D**).

Importantly, **MH1** interacts with DNA (**Figure 8A and B**), by binding to the minor groove of double-stranded DNA, as confirmed by DNA dye displacement assays and docking studies (**Figure 8C and D, Figure 10**). Finally, **MH1** inhibited human topoisomerase II $\alpha$  activity *in vitro* in a concentration dependent manner (**Figure 9A**). Being an important topoisomerase inside cells<sup>27</sup>, its inhibition resulted in G2/M arrest which was prominent at 6 and 12 h of **MH1** treatment in Molt4 cells. However, **MH1** did not interfere with topoisomerase I activity (**Figure 9B**). Besides topoisomerases, interaction of **MH1** with DNA resulted in inhibition of *in vitro* transcription explaining the mechanism of **MH1** action<sup>28</sup>. Thus our study identifies a novel benzimidazole derivative, **MH1** capable of binding to minor groove of DNA, thereby inhibiting crucial cellular processes and inducing intrinsic apoptotic pathway in leukemic cells leading to subsequent cell death.

Several benzimidazole derivatives were known to target DNA and associated processes<sup>1b</sup>. Consistent with this, the primary focus of the present study showed that novel benzimidazole derivative, **MH1** interacts with the minor groove of the DNA and inhibits several cellular processes. These observations open up several new avenues for further in depth studies.

Previously, certain benzimidazole derivatives were shown to interact specifically to G-quadruplex DNA structures<sup>29</sup>. Besides, G-quadruplex structures were shown to be one of the major reasons for DNA breakage during chromosomal translocations<sup>30</sup> and hence cancer progression. The important property of benzimidazole derivatives to bind G-quadruplex structure showed its significant role in inhibition of telomerase enzyme activity<sup>31</sup>, which is overexpressed in majority of cancers<sup>32</sup>.

Several known topoisomerase inhibitors like Etoposide or Doxorubicin are well studied for their ability to induce DNA damage and provoking DNA repair pathways and check point pathways <sup>27</sup>, however some benzimidazole derivatives induced cell cycle arrest as well as topoisomerase inhibition without causing DNA damage <sup>33</sup>. Therefore, further studies are required to address how these benzimidazole derivatives regulate signalling pathways which are important for cell cycle arrest and induction of apoptosis.

## MATERIALS AND METHODS

### CHEMISTRY

The progress of all reactions was monitored by TLC, which was performed on 2.0-5.0 cm aluminum sheets precoated with silica gel 60 F 254 to a thickness of 0.25 mm (Merck) using UV light for visualization. <sup>1</sup>H NMR and <sup>13</sup>C NMR spectra were recorded on an Agilent-varian NMR spectrometer operating at 400 and 100 MHz, respectively (**Supplementary figure 1a to n**). Chemical shifts are given in  $\delta$  values (ppm) using tetramethylsilane as the internal standard. Mass spectra were recorded using high resolution mass spectrometer (HRMS). Infrared spectra were recorded in KBr on Shimadzu FT-IR model 8300 spectrophotometer. Chromatographic separations were carried out on 60:120 silica gel.

#### 4-Bromo-1,2-diaminobenzene (2)

4-Bromo-2-nitro-aniline (5 mmol) and zinc dust (10 mmol) with catalytic amount of HCl was refluxed in ethanol (10 mL) for 3 h. The reaction mixture was filtered through celite and filtrate was evaporated under reduced pressure, the resulting residue was dissolved in ethylacetate and washed with water followed by brine solution. The organic layer was dried over anhydrous Na<sub>2</sub>SO<sub>4</sub> and evaporated under vacuo to obtain a desired amino product **2** as white solid <sup>34</sup>.

#### 5-bromo-2-p-tolyl-1H-benzimidazole (3)

T3P® (1.5 mmol, 50 % solution in ethylacetate) was added to the solution of 4-Bromo-1,2-diaminobenzene (1.0 mmol) and *p*-Tolualdehyde (1.0 mmol) in ethylacetate at 0°C and the resulting reaction mixture was stirred at room temperature for 2 h. The reaction mixture was diluted with water (20 mL) and neutralized with 10% NaHCO<sub>3</sub> solution and the product was extracted with ethyl acetate (10 mL X 2), the combined organic layer was washed with water followed by brine solution. The organic phase was dried over anhydrous Na<sub>2</sub>SO<sub>4</sub> and evaporated under reduced pressure to obtain a crude product, which was purified by column chromatography using ethyl acetate and hexane as an eluent to get the desired product **3** as a pale yellow solid. <sup>1</sup>H NMR (400 MHz, CDCl<sub>3</sub>): δ 8.32-8.30 (d, *J* = 8.0 Hz, 2H, ArH), 7.79 (br s, 1H, ArH), 7.38-7.36 (d, *J* = 7.6 Hz, 1H, ArH), 7.33-7.30 (dd, *J* = 8.4, 1.4 Hz, 1H, ArH), 7.29-7.27 (d, *J* = 7.8 Hz, 2H, ArH), 2.21 (s, 3H, Ar-CH<sub>3</sub>).

### **3,5-dibromobenzene-1,2-diamine (5)**

2,4-dibromo-6-nitroaniline (5 mmol) and zinc dust (10 mmol) with catalytic amount of HCl was refluxed in ethanol (10 mL) for 4 h. The reaction mixture was filtered through celite and filtrate was evaporated under reduced pressure, the resulting residue was dissolved in ethylacetate and washed with water followed by brine solution. The organic layer was dried over anhydrous Na<sub>2</sub>SO<sub>4</sub> and evaporated under vacuo to obtain 3,5-dibromobenzene-1,2-diamine (**5**) as a pale brown solid.

### **5,7-dibromo-2-*p*-tolyl-1H-benzimidazole (6) & 5,7-dibromo-2-(4-*tert*-butylphenyl)-1H-benzimidazole (7)**

Compounds **6** and **7** were synthesized as described earlier for the synthesis of **3** using *p*-Tolualdehyde and 4-*tert*-Butylbenzaldehyde as an aldehyde component to construct benzimidazole ring, respectively. **5,7-dibromo-2-*p*-tolyl-1H-benzimidazole (6)**; pale brown solid; <sup>1</sup>H NMR (400 MHz, CDCl<sub>3</sub>): δ 8.30-8.28 (d, *J* = 8.0 Hz, 2H, ArH), 7.81 (s, 1H, ArH), 7.64 (s, 1H, ArH), 7.31-7.29 (d, *J* = 8.2 Hz, 2H, ArH), 2.23 (s, 3H, Ar-CH<sub>3</sub>). **5,7-dibromo-2-(4-*tert*-butylphenyl)-1H-benzimidazole (7)**; dark brown solid; <sup>1</sup>H NMR (400 MHz, CDCl<sub>3</sub>): δ

8.29-8.27 (d,  $J = 8.2$  Hz, 2H, ArH), 7.80 (s, 1H, ArH), 7.62 (s, 1H, ArH), 7.33-7.31 (d,  $J = 8.0$  Hz, 2H, ArH), 1.51 (s, 9H, *t*-butyl-CH<sub>3</sub>).

### General procedure for the synthesis of title compounds MH1-5

Corresponding bromo compounds (3, 6 & 7) (1.0 mmol) were taken in water:Ethanol:1,4dioxane (6 mL) mixture in 1:1:5 ratio, potassium carbonate (3.0 mmol) and phenyl/4-bromo phenyl boronic acid (1.1 mmol) were added to the reaction mixture and degassed with nitrogen gas for 15 min with stirring at room temperature. Bis(triphenylphosphine)palladium(II) dichloride (0.1 mmol) catalyst was added to the mixture and heated for 30 min at 130°C in seal tube. The reaction mixture was filtered through celite and concentrated under reduced pressure, the resulting residue was diluted with ethylacetate and washed with water followed by brine solution. The organic layer was dried over anhydrous Na<sub>2</sub>SO<sub>4</sub> and concentrated under vacuo to give the crude product which was purified by column chromatography using hexane: ethylacetate as an eluent to get the title compounds (MH1-5).

### 5-phenyl-2-p-tolyl-1H-benzimidazole (MH1)

Yield: 84%; off white solid; m.p. 182-184 °C, IR  $\gamma_{\max}$  (KBr) 3350, 3154, 3123, 3087, 3030, 2980, 1380. cm<sup>-1</sup>; <sup>1</sup>H NMR (400 MHz, CDCl<sub>3</sub>);  $\delta$  8.00-7.98 (d,  $J = 8.0$  Hz, 2H, ArH), 7.78 (s, 1H, ArH), 7.68-7.66 (d,  $J = 8.0$  Hz, 1H, ArH), 7.62-7.59 (m, 2H, ArH), 7.51-7.49 (dd,  $J = 1.6$  Hz, 1H, ArH), 7.45-7.41 (m, 2H, ArH), 7.35-7.30 (m, 1H, ArH), 7.29-7.26 (m, 2H, ArH), 2.40 (s, 3H, Ar-CH<sub>3</sub>). <sup>13</sup>C NMR (100 MHz, CDCl<sub>3</sub>);  $\delta$  152.5, 141.7, 140.6, 136.5, 129.8, 128.7, 127.3, 126.9, 126.8, 126.5, 122.6, 120.8, 117.9, 21.4. HRMS (ESI)  $m/z$  Calcd for C<sub>20</sub>H<sub>16</sub>N<sub>2</sub>Na [M+Na]<sup>+</sup> 307.3544, found 307.3563.

### 5-(4-bromophenyl)-2-p-tolyl-1H-benzimidazole (MH2)

Yield: 78%; Brown solid; m.p. 184-186°C IR  $\gamma_{\max}$  (KBr) 3362, 3164, 3127, 3048, 2980, 1397, 550 cm<sup>-1</sup>; <sup>1</sup>H NMR (400 MHz, CDCl<sub>3</sub>);  $\delta$  7.97-7.92 (m, 2H, ArH), 7.75-7.68 (m,

1H, ArH), 7.67-7.64 (m, 2H, ArH), 7.58-7.56 (d,  $J = 9.6$  Hz, 1H, ArH), 7.53-7.51 (dd,  $J = 1.6$  Hz, 1H, ArH), 7.48-7.43 (m, 1H, ArH), 7.38-7.32 (m, 2H, ArH), 7.29-7.26 (m, 1H, ArH), 2.42 (s, 3H, Ar-CH<sub>3</sub>). **<sup>13</sup>C NMR (100 MHz, CDCl<sub>3</sub>);  $\delta$**  152.1, 141.9, 140.8, 136.4, 130.2, 129.9, 128.3, 127.9, 126.7, 126.1, 123.1, 122.8, 121.5, 117.7, 21.3. HRMS (ESI)  $m/z$  Calcd for C<sub>20</sub>H<sub>15</sub>BrN<sub>2</sub>Na [M+Na]<sup>+</sup> 386.2505, found 386.2531.

### 5,7-diphenyl-2-p-tolyl-1H-benzimidazole (MH3)

Yield: 82%; Pale brown solid; m.p. 166-168 °C, IR  $\gamma_{\max}$  (KBr) 3352, 3159, 3124, 3041, 2983, 1382 cm<sup>-1</sup>; **<sup>1</sup>H NMR (400 MHz, CDCl<sub>3</sub>);  $\delta$**  8.24-8.22 (d,  $J = 6.8$  Hz, 2H, ArH), 7.91-7.89 (d,  $J = 8.0$  Hz, 1H, ArH), 7.85 (s, 1H, ArH), 7.75 (s, 1H, ArH), 7.66-7.64 (d,  $J = 7.6$  Hz, 2H, ArH), 7.59-7.56 (m, 1H, ArH), 7.53-7.50 (t,  $J = 6.4$  Hz, 3H, ArH), 7.48-7.34 (m, 3H, ArH), 7.26-7.24 (t,  $J = 4.0$  Hz, 2H, ArH), 2.36 (s, 3H, Ar-CH<sub>3</sub>). **<sup>13</sup>C NMR (100 MHz, CDCl<sub>3</sub>);  $\delta$**  152.3, 135.8, 135.6, 134.7, 133.5, 132.6, 130.0, 129.8, 129.1, 128.8, 128.7, 128.5, 128.4, 128.2, 127.9, 127.4, 127.0, 126.7, 122.8, 22.7. HRMS (ESI)  $m/z$  Calcd for C<sub>26</sub>H<sub>20</sub>N<sub>2</sub>Na [M+Na]<sup>+</sup> 383.4504, found 383.4523.

### 5,7-bis(4-bromophenyl)-2-p-tolyl-1H-benzimidazole (MH4)

Yield: 75%; Dark brown solid; m.p. 91-93°C, IR  $\gamma_{\max}$  (KBr) 3401, 3213, 3178, 3102, 3032, 2997, 1396, 550, 542 cm<sup>-1</sup>; **<sup>1</sup>H NMR (400 MHz, CDCl<sub>3</sub>);  $\delta$**  7.99-7.90 (m, 2H, ArH), 7.71-7.69 (d,  $J = 7.2$  Hz, 3H, ArH), 7.56-7.50 (m, 4H, ArH), 7.49-7.45 (m, 2H, ArH), 7.37-7.33 (m, 3H, ArH), 2.16 (s, 3H, Ar-CH<sub>3</sub>). **<sup>13</sup>C NMR (100 MHz, CDCl<sub>3</sub>);  $\delta$**  152.6, 141.7, 140.5, 136.5, 132.0, 131.98, 131.93, 129.86, 129.81, 128.97, 128.90, 128.65, 128.60, 128.0, 127.5, 127.4, 126.7, 126.6, 21.4. HRMS (ESI)  $m/z$  Calcd for C<sub>26</sub>H<sub>18</sub>Br<sub>2</sub>N<sub>2</sub>Na [M+Na]<sup>+</sup> 541.2425, found 541.2442.

### 2-(4-tert-butylphenyl)-5,7-diphenyl-1H-benzimidazole (MH5)

Yield: 81%; Off white solid; m.p. 198-200°C, IR  $\gamma_{\max}$  (KBr) 3399, 3202, 3165, 3114, 2997, 2984, 1395, 1387 cm<sup>-1</sup>; **<sup>1</sup>H NMR (400 MHz, CDCl<sub>3</sub>);  $\delta$**  7.97-7.87 (m, 4H, ArH), 7.80-



7.70 (m, 3H, ArH), 7.68-7.63 (m, 2H, ArH), 7.62-7.51 (m, 4H, ArH), 7.31-7.28 (m, 3H, ArH), 1.25 (s, 9H, *t*-butyl-CH<sub>3</sub>). <sup>13</sup>C NMR (100 MHz, CDCl<sub>3</sub>); δ 152.5, 135.5, 134.7, 133.5, 132.4, 130.0, 129.4, 129.2, 128.8, 128.7, 128.5, 128.1, 127.9, 127.8, 127.6, 127.0, 126.7, 124.6, 31.1, 30.9. HRMS (ESI) *m/z* Calcd for C<sub>29</sub>H<sub>26</sub>N<sub>2</sub>Na [M+Na]<sup>+</sup> 425.5301, found 425.5312.

## BIOLOGY

### Chemicals and reagents

All the chemicals used in the present study were of analytical grade and purchased from Sigma-Aldrich, USA. Human Topoisomerase I and II $\alpha$  were purchased from TopoGEN.Inc, USA. DNA modifying enzymes were from New England Biolabs (USA). Antibodies were from Santacruz Biotechnology or Invitrogen (USA).

### Cell culture

Human cancer cell lines, Molt4 (acute lymphoblastic leukemia), K562 (Chronic myelogenous leukemia), EAC (Mouse breast cancer), MCF7 (Human breast cancer) and HeLa (Human cervical cancer) were purchased from National Centre for Cell Science, Pune, India and Nalm6 (B-cell leukemia) and REH (B-cell leukemia) were a kind gift from Dr. M.R. Lieber, USA. Cells were cultured in RPMI1640, MEM or DMEM (Sera Lab, UK) containing 10% FBS (Gibco BRL, USA), 100 U of Penicillin G/ml and 100  $\mu$ g of streptomycin/ml (Sigma–Aldrich, USA) at 37°C in a humidified atmosphere containing 5% CO<sub>2</sub>.

### MTT assay

Cytotoxic effect of newly synthesized benzimidazole derivatives was studied using MTT assay <sup>35</sup>. Briefly, leukemic cell lines were seeded in a 24 well plate at a density of 50,000 cells/ml and treated with different concentrations (0-40  $\mu$ M) of synthesized compounds for 48 or 72 h. 100  $\mu$ l of cell suspension from each sample was mixed with 10  $\mu$ l of MTT (5 mg/ml) in 96 well plate, incubated for 2-3 h, formazone crystals were solubilized in 67  $\mu$ l of solution containing 10% SDS and 50% DMF (30-60 min at 37°C) and readings were

acquired at 570 nm using Biorad iMARK (USA) plate reader. Adherent cell lines (MCF7, HeLa and EAC), were seeded directly in 96 well plate at the density of 5000 cells/well and incubated with different concentrations (0-40  $\mu$ M) of compounds and subjected to MTT assay as described above. Experiments were repeated a minimum of two times with good agreement, each with duplicate reactions and bar diagram is presented with error bars. IC<sub>50</sub> values were determined using GraphPad software prism 5.1.

### Cell cycle analysis

To study the effect of **MH1** on cell cycle progression in Molt4 and K562 cells, cells were seeded at a density of 50,000 cells/ml, and treated with different concentrations of **MH1** (0, 1, 5, 10 and 20  $\mu$ M) for 48 h as described previously<sup>36</sup>. Besides, Molt4 cells were treated with **MH1** (10  $\mu$ M) for different time points (3, 6, 12 and 24 h). DMSO treated cells were served as a vehicle control. For cell cycle analysis, following MH1 treatment, cells were harvested, washed in 1x PBS and fixed with 80% chilled ethanol. Fixed cells were subjected to RNase A treatment (50  $\mu$ g/ml, at 37°C for 4-12 h. Cells were stained with propidium iodide (10  $\mu$ g/ml) and analysed in BD FACSVerse™. Minimum 10,000 cells were acquired and analysed in Flowing software (version2.5). Experiments were repeated a minimum of two independent times and presented as histogram and % of cells in different phases of cell cycle are presented as bar diagram with error bars.

### Annexin-FITC/ PI staining

Induction of apoptosis following **MH1** treatment in Molt4 cells was studied using Annexin-FITC/PI staining kit (Santacruz, USA)<sup>37</sup>. Briefly, different concentrations of **MH1** (0, 1, 5 and 10  $\mu$ M) were incubated with Molt4 cells (50,000 cells/ml) for 48 h. Cells were harvested, suspended in binding buffer containing calcium along with Annexin-FITC (0.2 mg/ml) and propidium iodide (50 ng/ml) for 20 min at room temperature and was analysed on BD FACSVerse™. Minimum 10,000 cells were acquired per sample and analysed in Flowing software (version 2.5). DMSO treated cells were used as a vehicle control.

Experiments were repeated a minimum of two times and results were presented as dot plots. % cells in early, late apoptosis and necrosis are presented as a bar diagram with error bars.

For confocal microscopy, Annexin-FITC/PI stained cells were fixed using 2% paraformaldehyde for 15 min at room temperature. Cells were washed with 1x PBS and mounted on slides using DABCO. Images were captured using inverted confocal laser scanning microscope (Zeiss LSM 510 MK4, Germany).

### **Live dead cell assay**

Effect of **MH1** on Molt4 cell viability was also analysed by performing live dead cell assay using calcein-AM and ethidium homodimer staining <sup>38</sup>. Briefly, Molt4 cells were incubated with increasing concentrations of **MH1** (0, 1, 5 and 10  $\mu$ M) for 48 h. Cells were harvested, washed in 1x PBS and incubated with calcein-AM (100 nM) and ethidium homodimer (8  $\mu$ M) for 20 min at 37°C and analysed in BD FACSVerse™ (10,000 cells per sample). DMSO treated cells were used as a vehicle control. Data are presented as dot plots. Cells stained with calcein-AM alone (live cells) or ethidium homodimer alone (dead cells) or both are presented as a bar diagram with error bars.

### **DNA fragmentation assay**

DNA fragmentation during apoptotic induction by **MH1** on Molt4 cells was studied using DNA fragmentation assay <sup>20b</sup>. Briefly, Molt4 cells were incubated with increasing concentrations of **MH1** (0, 1, 5, 10 and 20  $\mu$ M for 48 h), harvested, washed in PBS and lysed in lysis buffer (100 mM NaCl, 10 mM Tris pH 8.0, 0.25% Triton X-100, 1mM EDTA and 100  $\mu$ g/ml Proteinase K for 4 h at 55°C). Following RNase treatment (50  $\mu$ g/ml, for 1 h at 37°C), and deproteinization (phenol: chloroform extraction), DNA was precipitated, washed with 70% ethanol, dried and dissolved in TE. DNA concentration was estimated, and equal concentration was loaded on 2% agarose gel and electrophoresed at 50V for 3 h. DNA hyper ladder I was used as a marker to assess the length of the DNA. Quantification of

HMW (high molecular weight) DNA and fragmented DNA was carried out using Multi Gauge V3.0 software and presented as a bar diagram with error bars (n=2).

### Measurement of mitochondrial membrane potential assay

To test the involvement of mitochondrial machinery in induction of apoptosis, JC-1 staining was carried out<sup>39</sup>. Briefly, Molt4 cells treated with different concentrations of **MH1** (0, 1, 5, 10 and 20  $\mu$ M) were harvested at 48 h, incubated with JC-1 dye (5, 5', 6, 6'-tetrachloro-1, 1, 3, 3'-tetraethylbenzimidazolcarbocyanamide iodided; 2  $\mu$ M; Calbiochem, USA) for 30 min at 37°C, washed and immediately analysed in BD FACSVerse™. Cells treated with 2, 4-DNP was used as a positive control, and cells treated with DMSO alone was served as a vehicle control. Data are presented as dot plots, percentage cells with high, intermediate and low mitochondrial membrane potential (MMP) are presented in bar diagram with error bars based on minimum of two experiments.

### Western blot analysis

Effect of **MH1** on the expression of apoptotic proteins was analysed on Molt4 cells following **MH1** treatment by western blot analysis. Cell lysate was prepared after 48 h of **MH1** treatment (0, 1, 5 and 10  $\mu$ M) using RIPA buffer method as described previously<sup>40</sup>. ~30  $\mu$ g of protein from each sample was resolved on a SDS-PAGE (12%), transferred to PVDF membrane (Millipore, USA) and probed with respective primary, biotinylated secondary and streptavidin HRP antibodies. The primary antibodies used were BAX, BCL2, and Actin (from Invitrogen, USA); CASPASE9 and CASPASE3 (from Santacruz, USA). Membranes were developed using chemiluminescent reagents (Bio-Rad, USA) and imaged were acquired using gel documentation system (LAS 3000, Fuji, Japan). Actin served as loading control. Quantification of the western blots were carried out using Multi Gauge V3.0 software and presented as a bar diagram in fold changes with respect to the control with error bars (n=2).

### Molecular docking studies

2D structure of **MH1** was sketched in ChemBioDraw Ultra 14.0. Explicit hydrogen were added and converted into 3D structure using Open Babel 2.3.2<sup>41</sup> (<http://openbabel.org>). 3D crystal structure of double stranded DNA bound with Hoechst 33258 at minor groove was retrieved from protein databank (PDB ID: 127D, [www.rcsb.org/pdb](http://www.rcsb.org/pdb)). Molecular docking studies were carried out with Autodock4.2 program<sup>42</sup>. Briefly, ligand was removed from the DNA PDB structure and PDBQT files were generated for DNA molecule and **MH1**. Grid files were created keeping the grid centres 15, 21.23 and 8.45 on X, Y and Z dimensions, respectively (npts= 60 for X, Y and Z, spacing= 0.375). Rigid docking was carried out using Lamarckian genetic algorithm (GA run was kept 25 with long search parameter). Best pose was selected according to lower binding energy and presented in the final image. Images were created with PyMOL (<http://www.pymol.org/>).

### **MH1-DNA interaction studies**

DNA interaction studies were carried out using Calf thymus (CT) DNA (Sigma) dissolved in 20 mM Tris-HCl, pH 7.4 with 15 mM NaCl and 0.5 mM EDTA (all the assays were performed using same buffer). Concentration of CT-DNA was determined by UV-spectroscopy using the extinction coefficient  $12824 \text{ M}^{-1} \text{ cm}^{-1}$ .

### **UV-VIS spectroscopy**

**MH1**-DNA interaction studies were carried out using UV-VIS spectrometer (Perkin Elmer, Lambda 35)<sup>43</sup>. Briefly, **MH1** (10  $\mu\text{M}$ ) was scanned (200 nm to 550 nm) with different concentration of CT-DNA (0, 1, 5, 10, 25, 50, 75 and 100  $\mu\text{M}$ ) with a scan speed of 240 nm/min, three cycles keeping the scan intervals of 0.5 nm and 2 nm slit width. Resulting absorbance (A) was plotted with the function of wavelength.

### **Fluorescence emission spectrum measurement**

Fluorescence emission studies<sup>44</sup> of **MH1**-DNA interactions were carried out in 96 well plate microplate reader Infinite M200PRO (Tecan Group Ltd., Switzerland). Briefly, 1  $\mu\text{M}$

**MH1** was added with the different concentration of CT-DNA (0, 1, 5, 10, 25, 50, 75 and 100  $\mu\text{M}$ ) and scanned for the emission spectra from 300 to 550 nm at 259 nm excitation range (Instrument settings: z-position- 20000  $\mu\text{m}$ , gain-100, integration time- 20  $\mu\text{s}$  and number of flashes-25 with 1 nm step). Resulting fluorescence intensity (RFU) is plotted as the function of wavelength.

### DNA dye displacement assay

To check the mode of **MH1** binding to DNA, we have carried out DNA dye displacement assay using Hoechst 33258 or Ethidium bromide dye <sup>45</sup>. Briefly, 20  $\mu\text{M}$  CT-DNA along with 5  $\mu\text{M}$  Hoechst 33258 was incubated with different concentration of **MH1** (0, 1, 5, 10, 25, 50 and 100  $\mu\text{M}$ ) for 10 min at room temperature, emission spectra was scanned from 400 to 650 nm at excitation of 352 nm. 50  $\mu\text{M}$  **MH3** was also used to check its ability to displace the Hoechst as it showed poor cytotoxicity *ex vivo*. Fluorescence intensity from compound alone was also measured and used for the subsequent subtraction in the final graph. Similarly, ethidium bromide (1  $\mu\text{M}$ ) displacement assay was also carried out (emission range from 530 to 780 at 510 nm excitation) and emission spectra was plotted as described previously.

### Circular dichroism

In order to check the DNA topological changes upon binding with **MH1**, circular dichroism studies were performed <sup>46</sup>. Calf thymus DNA (50  $\mu\text{M}$ ) was incubated with different concentrations of **MH1** (0, 10, 25, 50 and 100  $\mu\text{M}$ ) and circular dichroism (CD) spectra were recorded at room temperature from 220 to 300 nm with five cycles for every sample using a JASCO J-810 spectropolarimeter (scan speed of 100 nm/min). Buffer with compound alone was subtracted from corresponding spectra and final graph was presented. Hoechst 33258 (10  $\mu\text{M}$ ) was used as a positive control.

### Topoisomerase assay

Ability of **MH1** to inhibit topoisomerase activity was checked using recombinant human topoisomerase I and human topoisomerase II  $\alpha$  (TopoGEN.Inc, USA). Supercoiled plasmid DNA (pBS-SK+) was isolated using GenElute plasmid miniprep kit (Sigma), according to the manufactures instructions. ~250 ng of plasmid DNA was incubated with different concentrations of **MH1** (0, 10, 25, 50 and 100  $\mu$ M, at RT for 5 min; equal amount of DMSO was added in controls). To this, topoisomerase enzyme (2 units) was added in the supplied reaction buffer (30 min incubation at 37°C). Reactions were terminated by addition of stop buffer containing 5% sarkosyl, 0.125% bromophenol blue, 25% glycerol and resolved on 0.8 % agarose gel (40 v, 4 h). Following ethidium bromide post staining, gel images were captured. Etoposide (100  $\mu$ M) and Topotecan (7.5  $\mu$ M) were served as a positive control for topoisomerase II  $\alpha$  and topoisomerase I, respectively. Experiments were carried out a minimum of two independent times.

### ***In vitro* transcription assay**

To have an insight on other DNA related activities, we performed *in vitro* transcription assay using T7 RNA polymerase (NEB, USA)<sup>47</sup>. Briefly, 500 ng of pBS-SK+ plasmid DNA was incubated with different concentrations of **MH1** (0, 10, 25, 50 and 100  $\mu$ M) at room temperature for 5 min (equal amount of DMSO was added in the control reactions), in presence T7 RNA polymerase (5 units). Reactions were incubated for 30 min at 37°C, terminated and further processed as described above in “topoisomerase assay”. RNase A (50  $\mu$ g/ml) was used to confirm the synthesised RNA species.

### **Statistical analysis**

The error bars were expressed as mean  $\pm$  SEM. Statistical analysis was performed using One-way ANOVA followed by Dunnett test and significance was calculated after comparing each value with control using GraphPad software prism 5.1. The values were considered as statistically significant, if the p-value was equal to or less than 0.05 (0.05\*, 0.005\*\*, 0.0005\*\*\*).

## ACKNOWLEDGEMENTS

We thank Dr. M. Nambiar and other members of SCR laboratory for discussions and comments on the manuscript. We thank NMR, Confocal and FACS facility at IISc for their help. This work was supported by grants from DST (F.NO.SR/SO/HS-006/2010 (G) Dated 29.08.2011) to KSR and SCR, IISc-DBT partnership programme [DBT/BF/PR/INS/2011-12/IISc] to SCR. MH is supported by Junior Research Fellowship from DST-PURSE program.

## Conflict of interest

Authors disclose that there is no conflict of interest.

## References

- (a) Moen, M. D.; McKeage, K.; Plosker, G. L.; Siddiqui, M. A., Imatinib: a review of its use in chronic myeloid leukaemia. *Drugs* **2007**, *67* (2), 299-320; (b) Paul, A.; Bhattacharya, S., Chemistry and biology of DNA-binding small molecules. *Curr. Sci.* **2012**, *102* (2).
- (a) Henderson, D.; Hurley, L. H., Molecular struggle for transcriptional control. *Nat. Med.* **1995**, *1* (6), 525-7; (b) Hurley, L. H., DNA and its associated processes as targets for cancer therapy. *Nat. Rev. Cancer* **2002**, *2* (3), 188-200; (c) Anthoney, D. A.; Twelves, C. J., DNA: still a target worth aiming at? A review of new DNA-interactive agents. *Am. J. Pharmacogenomics* **2001**, *1* (1), 67-81.
- Cai, X.; Gray, P. J., Jr.; Von Hoff, D. D., DNA minor groove binders: back in the groove. *Cancer Treat. Rev.* **2009**, *35* (5), 437-50.
- (a) Lown, J. W., DNA recognition by lexitropsins, minor groove binding agents. *J. Mol. Recognit.* **1994**, *7* (2), 79-88; (b) Reddy, B. S.; Sondhi, S. M.; Lown, J. W., Synthetic DNA minor groove-binding drugs. *Pharmacol. Ther.* **1999**, *84* (1), 1-111.
- (a) Mann, J.; Baron, A.; Opoku-Boahen, Y.; Johansson, E.; Parkinson, G.; Kelland, L. R.; Neidle, S., A new class of symmetric bisbenzimidazole-based DNA minor groove-binding agents showing antitumor activity. *J. Med. Chem.* **2001**, *44* (2), 138-44; (b) Helal, M. H.; Al-Mudaris, Z. A.; Al-Douh, M. H.; Osman, H.; Wahab, H. A.; Alnajjar, B. O.; Abdallah, H. H.; Abdul Majid, A. M., Diaminobenzene schiff base, a novel class of DNA minor groove binder. *Int. J. Oncol.* **2012**, *41* (2), 504-10; (c) Al-Mudaris, Z. A.; Majid, A. S.; Ji, D.; Al-Mudarris, B. A.; Chen, S. H.; Liang, P. H.; Osman, H.; Jamal Din, S. K.; Abdul Majid, A. M., Conjugation of benzylvanillin and benzimidazole structure improves DNA binding with enhanced



- antileukemic properties. *PLoS One* **2013**, *8* (11), e80983; (d) Vidal, A.; Munoz, C.; Guillen, M. J.; Moreto, J.; Puertas, S.; Martinez-Iñiesta, M.; Figueras, A.; Padullés, L.; Garcia-Rodriguez, F. J.; Berdiel-Acer, M.; Pujana, M. A.; Salazar, R.; Gil-Martin, M.; Marti, L.; Ponce, J.; Mollevi, D. G.; Capella, G.; Condom, E.; Vinals, F.; Huertas, D.; Cuevas, C.; Esteller, M.; Aviles, P.; Villanueva, A., Lurbinectedin (PM01183), a new DNA minor groove binder, inhibits growth of orthotopic primary graft of cisplatin-resistant epithelial ovarian cancer. *Clin. Cancer Res.* **2012**, *18* (19), 5399-411; (e) Fedier, A.; Fowst, C.; Tursi, J.; Geroni, C.; Haller, U.; Marchini, S.; Fink, D., Brostallicin (PNU-166196)--a new DNA minor groove binder that retains sensitivity in DNA mismatch repair-deficient tumour cells. *Br. J. Cancer* **2003**, *89* (8), 1559-65; (f) Neidle, S., DNA minor-groove recognition by small molecules. *Nat. Prod. Rep.* **2001**, *18* (3), 291-309.
6. Hamilton, P. L.; Arya, D. P., Natural product DNA major groove binders. *Nat. Prod. Rep.* **2012**, *29* (2), 134-43.
7. Brosh, R. M., Jr.; Karow, J. K.; White, E. J.; Shaw, N. D.; Hickson, I. D.; Bohr, V. A., Potent inhibition of werner and bloom helicases by DNA minor groove binding drugs. *Nucleic Acids Res.* **2000**, *28* (12), 2420-30.
8. (a) Beerman, T. A.; McHugh, M. M.; Sigmund, R.; Lown, J. W.; Rao, K. E.; Bathini, Y., Effects of analogs of the DNA minor groove binder Hoechst 33258 on topoisomerase II and I mediated activities. *Biochim. Biophys. Acta* **1992**, *1131* (1), 53-61; (b) Woynarowski, J. M.; McHugh, M.; Sigmund, R. D.; Beerman, T. A., Modulation of topoisomerase II catalytic activity by DNA minor groove binding agents distamycin, Hoechst 33258, and 4',6-diamidine-2-phenylindole. *Mol. Pharmacol.* **1989**, *35* (2), 177-82.
9. (a) Garuti, L.; Roberti, M.; Bottegoni, G., Benzimidazole derivatives as kinase inhibitors. *Curr. Med. Chem.* **2014**, *21* (20), 2284-98; (b) Velagapudi, S. P.; Seedhouse, S. J.; French, J.; Disney, M. D., Defining the RNA internal loops preferred by benzimidazole derivatives via 2D combinatorial screening and computational analysis. *J. Am. Chem. Soc.* **2011**, *133* (26), 10111-8.
10. Demirayak, S.; Abu Mohsen, U.; Cagri Karaburun, A., Synthesis and anticancer and anti-HIV testing of some pyrazino[1,2-a]benzimidazole derivatives. *Eur. J. Med. Chem.* **2002**, *37* (3), 255-60.
11. Ayhan-Kilcigil, G.; Kus, C.; Coban, T.; Can-Eke, B.; Iscan, M., Synthesis and antioxidant properties of novel benzimidazole derivatives. *Enzyme Inhib. Med. Chem.* **2004**, *19* (2), 129-35.
12. Sharma, D.; Narasimhan, B.; Kumar, P.; Judge, V.; Narang, R.; De Clercq, E.; Balzarini, J., Synthesis, antimicrobial and antiviral activity of substituted benzimidazoles. *Enzyme Inhib. Med. Chem.* **2009**, *24* (5), 1161-8.

13. Emery, V. C.; Hassan-Walker, A. F., Focus on new drugs in development against human cytomegalovirus. *Drugs* **2002**, *62* (13), 1853-8.
14. Kumar, B. V.; Vaidya, S. D.; Kumar, R. V.; Bhirud, S. B.; Mane, R. B., Synthesis and anti-bacterial activity of some novel 2-(6-fluorochroman-2-yl)-1-alkyl/acyl/aroyl-1H-benzimidazoles. *Eur. J. Med. Chem.* **2006**, *41* (5), 599-604.
15. (a) Kazimierczuk, Z.; Andrzejewska, M.; Kaustova, J.; Klimesova, V., Synthesis and antimycobacterial activity of 2-substituted halogenobenzimidazoles. *Eur. J. Med. Chem.* **2005**, *40* (2), 203-8; (b) Stanley, S. A.; Grant, S. S.; Kawate, T.; Iwase, N.; Shimizu, M.; Wivagg, C.; Silvis, M.; Kazyanskaya, E.; Aquadro, J.; Golas, A.; Fitzgerald, M.; Dai, H.; Zhang, L.; Hung, D. T., Identification of novel inhibitors of *M. tuberculosis* growth using whole cell based high-throughput screening. *ACS Chem. Biol.* **2012**, *7* (8), 1377-84.
16. (a) Penning, T. D.; Zhu, G. D.; Gandhi, V. B.; Gong, J.; Liu, X.; Shi, Y.; Klinghofer, V.; Johnson, E. F.; Donawho, C. K.; Frost, D. J.; Bontcheva-Diaz, V.; Bouska, J. J.; Osterling, D. J.; Olson, A. M.; Marsh, K. C.; Luo, Y.; Giranda, V. L., Discovery of the Poly(ADP-ribose) polymerase (PARP) inhibitor 2-[(R)-2-methylpyrrolidin-2-yl]-1H-benzimidazole-4-carboxamide (ABT-888) for the treatment of cancer. *J. Med. Chem.* **2009**, *52* (2), 514-23; (b) Hao, D.; Rizzo, J. D.; Stringer, S.; Moore, R. V.; Marty, J.; Dexter, D. L.; Mangold, G. L.; Camden, J. B.; Von Hoff, D. D.; Weitman, S. D., Preclinical antitumor activity and pharmacokinetics of methyl-2-benzimidazolecarbamate (FB642). *Invest. New. Drugs.* **2002**, *20* (3), 261-70; (c) Refaat, H. M., Synthesis and anticancer activity of some novel 2-substituted benzimidazole derivatives. *Eur. J. Med. Chem.* **2010**, *45* (7), 2949-56; (d) Abonia, R.; Cortes, E.; Insuasty, B.; Quiroga, J.; Nogueras, M.; Cobo, J., Synthesis of novel 1,2,5-trisubstituted benzimidazoles as potential antitumor agents. *Eur. J. Med. Chem.* **2011**, *46* (9), 4062-70.
17. Chaudhuri, P.; Ganguly, B.; Bhattacharya, S., An experimental and computational analysis on the differential role of the positional isomers of symmetric bis-2-(pyridyl)-1H-benzimidazoles as DNA binding agents. *J. Org. Chem.* **2007**, *72* (6), 1912-23.
18. Bhattacharya, S.; Chaudhuri, P., Medical implications of benzimidazole derivatives as drugs designed for targeting DNA and DNA associated processes. *Curr. Med. Chem.* **2008**, *15* (18), 1762-77.
19. (a) Raghavendra, G. M.; Ramesha, A. B.; Revanna, C. N.; Nandeesh, K. N.; Mantelingu, K.; Rangappa, K. S., One-pot tandem approach for the synthesis of benzimidazoles and benzothiazoles from alcohols. *Tetrahedron Lett.* **2011**, *52* (43), 5571-5574; (b) Sharath Kumar, K. S.; Swaroop, T. R.; Harsha, K. B.; Narasimhamurthy, K. H.; Rangappa, K. S., T3P®-DMSO mediated one pot cascade protocol for the synthesis of 4-thiazolidinones from alcohols. *Tetrahedron Lett.* **2012**, *53* (42), 5619-5623.

20. (a) Collins, J. A.; Schandi, C. A.; Young, K. K.; Vesely, J.; Willingham, M. C., Major DNA fragmentation is a late event in apoptosis. *J. Histochem. Cytochem.* **1997**, *45* (7), 923-34; (b) Kumar, S.; Hegde, M.; Gopalakrishnan, V.; Renuka, V. K.; Ramareddy, S. A.; De Clercq, E.; Schols, D.; Gudibabande Narasimhamurthy, A. K.; Raghavan, S. C.; Karki, S. S., 2-(4-Chlorobenzyl)-6-arylimidazo[2,1-b][1,3,4]thiadiazoles: synthesis, cytotoxic activity and mechanism of action. *Eur. J. Med. Chem.* **2014**, *84*, 687-97.
21. Gottlieb, E.; Armour, S. M.; Harris, M. H.; Thompson, C. B., Mitochondrial membrane potential regulates matrix configuration and cytochrome c release during apoptosis. *Cell Death Differ.* **2003**, *10* (6), 709-17.
22. Tu, L. C.; Chen, C. S.; Hsiao, I. C.; Chern, J. W.; Lin, C. H.; Shen, Y. C.; Yeh, S. F., The beta-carboline analog Mana-Hox causes mitotic aberration by interacting with DNA. *Chem. Biol.* **2005**, *12* (12), 1317-24.
23. Shahabadi, N.; Maghsudi, M., Multi-spectroscopic and molecular modeling studies on the interaction of antihypertensive drug; methyldopa with calf thymus DNA. *Mol. Biosyst.* **2014**, *10* (2), 338-47.
24. Tse, W. C.; Boger, D. L., A fluorescent intercalator displacement assay for establishing DNA binding selectivity and affinity. *Curr. Protoc. Nucleic Acid Chem.* **2005**, Chapter 8, Unit 8 5.
25. (a) Pilch, D. S.; Xu, Z.; Sun, Q.; Lavoie, E. J.; Liu, L. F.; Geacintov, N. E.; Breslauer, K. J., Characterizing the DNA binding modes of a topoisomerase I-poisoning terbenzimidazole: evidence for both intercalative and minor groove binding properties. *Drug. Des. Discov.* **1996**, *13* (3-4), 115-33; (b) Portugal, J., Berenil acts as a poison of eukaryotic topoisomerase II. *FEBS Lett.* **1994**, *344* (2-3), 136-8.
26. Majumder, P.; Banerjee, A.; Shandilya, J.; Senapati, P.; Chatterjee, S.; Kundu, T. K.; Dasgupta, D., Minor groove binder distamycin remodels chromatin but inhibits transcription. *PLoS One* **2013**, *8* (2), e57693.
27. Nitiss, J. L., Targeting DNA topoisomerase II in cancer chemotherapy. *Nat. Rev. Cancer* **2009**, *9* (5), 338-50.
28. Zihlif, M.; Catchpoole, D. R.; Stewart, B. W.; Wakelin, L. P., Effects of DNA minor groove binding agents on global gene expression. *Cancer Genomics Proteomics.* **2010**, *7* (6), 323-30.
29. (a) Maji, B.; Bhattacharya, S., Advances in the molecular design of potential anticancer agents via targeting of human telomeric DNA. *Chem. Commun.* **2014**, *50* (49), 6422-38; (b) Maji, B.; Bhattacharya, S., Molecular design of synthetic benzimidazoles for the switchover of the duplex to G-quadruplex DNA recognition. *Chimia* **2013**, *67* (1-2), 39-43.

30. (a) Nambiar, M.; Srivastava, M.; Gopalakrishnan, V.; Sankaran, S. K.; Raghavan, S. C., G-quadruplex structures formed at the HOX11 breakpoint region contribute to its fragility during t(10;14) translocation in T-cell leukemia. *Mol. Cell. Biol.* **2013**, *33* (21), 4266-81; (b) Nambiar, M.; Goldsmith, G.; Moorthy, B. T.; Lieber, M. R.; Joshi, M. V.; Choudhary, B.; Hosur, R. V.; Raghavan, S. C., Formation of a G-quadruplex at the BCL2 major breakpoint region of the t(14;18) translocation in follicular lymphoma. *Nucleic Acids Res.* **2011**, *39* (3), 936-48; (c) Katapadi, V. K.; Nambiar, M.; Raghavan, S. C., Potential G-quadruplex formation at breakpoint regions of chromosomal translocations in cancer may explain their fragility. *Genomics* **2012**, *100* (2), 72-80.
31. (a) Bhattacharya, S.; Chaudhuri, P.; Jain, A. K.; Paul, A., Symmetrical bisbenzimidazoles with benzenediyl spacer: the role of the shape of the ligand on the stabilization and structural alterations in telomeric G-quadruplex DNA and telomerase inhibition. *Bioconjug. Chem.* **2010**, *21* (7), 1148-59; (b) Jain, A. K.; Reddy, V. V.; Paul, A.; K, M.; Bhattacharya, S., Synthesis and evaluation of a novel class of G-quadruplex-stabilizing small molecules based on the 1,3-phenylene-bis(piperazinyl benzimidazole) system. *Biochemistry* **2009**, *48* (45), 10693-704; (c) Jain, A. K.; Paul, A.; Maji, B.; Muniyappa, K.; Bhattacharya, S., Dimeric 1,3-phenylene-bis(piperazinyl benzimidazole)s: synthesis and structure-activity investigations on their binding with human telomeric G-quadruplex DNA and telomerase inhibition properties. *J. Med. Chem.* **2012**, *55* (7), 2981-93.
32. Cech, T. R., Life at the End of the Chromosome: Telomeres and Telomerase. *Angew. Chem. Int. Ed. Engl.* **2000**, *39* (1), 34-43.
33. Kim, S. O.; Sakchaisri, K.; Thimmegowda, N. R.; Soung, N. K.; Jang, J. H.; Kim, Y. S.; Lee, K. S.; Kwon, Y. T.; Asami, Y.; Ahn, J. S.; Erikson, R. L.; Kim, B. Y., STK295900, a dual inhibitor of topoisomerase 1 and 2, induces G(2) arrest in the absence of DNA damage. *PLoS One* **2013**, *8* (1), e53908.
34. Rangarajan, M.; Kim, J. S.; Sim, S. P.; Liu, A.; Liu, L. F.; Lavoie, E. J., Topoisomerase I inhibition and cytotoxicity of 5-bromo- and 5-phenylterbenzimidazoles. *Bioorg. Med. Chem.* **2000**, *8* (11), 2591-600.
35. Hegde, M.; Karki, S. S.; Thomas, E.; Kumar, S.; Panjamurthy, K.; Ranganatha, S. R.; Rangappa, K. S.; Choudhary, B.; Raghavan, S. C., Novel levamisole derivative induces extrinsic pathway of apoptosis in cancer cells and inhibits tumor progression in mice. *PLoS One* **2012**, *7* (9), e43632.
36. (a) Srivastava, M.; Hegde, M.; Chiruvella, K. K.; Korothe, J.; Bhattacharya, S.; Choudhary, B.; Raghavan, S. C., Sapodilla plum (*Achras sapota*) induces apoptosis in cancer cell lines and inhibits tumor progression in mice. *Sci. Rep.* **2014**, *4*, 6147; (b) Kavitha, C. V.; Nambiar, M.; Ananda Kumar, C. S.; Choudhary, B.; Muniyappa, K.; Rangappa, K. S.;

- Raghavan, S. C., Novel derivatives of spirohydantoin induce growth inhibition followed by apoptosis in leukemia cells. *Biochem. Pharmacol.* **2009**, *77* (3), 348-63.
37. Chiruvella, K. K.; Kari, V.; Choudhary, B.; Nambiar, M.; Ghanta, R. G.; Raghavan, S. C., Methyl angolensate, a natural tetranortriterpenoid induces intrinsic apoptotic pathway in leukemic cells. *FEBS Lett.* **2008**, *582* (29), 4066-76.
38. Kummrow, A.; Frankowski, M.; Bock, N.; Werner, C.; Dziekan, T.; Neukammer, J., Quantitative assessment of cell viability based on flow cytometry and microscopy. *Cytometry A.* **2013**, *83* (2), 197-204.
39. Kumar, S.; Gopalakrishnan, V.; Hegde, M.; Rana, V.; Dhepe, S. S.; Ramareddy, S. A.; Leoni, A.; Locatelli, A.; Morigi, R.; Rambaldi, M.; Srivastava, M.; Raghavan, S. C.; Karki, S. S., Synthesis and antiproliferative activity of imidazo[2,1-b][1,3,4]thiadiazole derivatives. *Bioorg. Med. Chem. Lett.* **2014**, *24* (19), 4682-8.
40. Somasagara, R. R.; Hegde, M.; Chiruvella, K. K.; Musini, A.; Choudhary, B.; Raghavan, S. C., Extracts of strawberry fruits induce intrinsic pathway of apoptosis in breast cancer cells and inhibits tumor progression in mice. *PLoS One* **2012**, *7* (10), e47021.
41. O'Boyle, N. M.; Banck, M.; James, C. A.; Morley, C.; Vandermeersch, T.; Hutchison, G. R., Open Babel: An open chemical toolbox. *J. Cheminform.* **2011**, *3*, 33.
42. Morris, G. M.; Huey, R.; Lindstrom, W.; Sanner, M. F.; Belew, R. K.;Goodsell, D. S.; Olson, A. J., AutoDock4 and AutoDockTools4: Automated docking with selective receptor flexibility. *J. Comput. Chem.* **2009**, *30* (16), 2785-91.
43. Shahabuddin, M. S.; Gopal, M.; Raghavan, S. C., Intercalating, cytotoxic, antitumor activity of 8-chloro and 4-morpholinopyrimido [4',5':4,5]thieno(2,3-b)quinolines. *J. Photochem. Photobiol. B.* **2009**, *94* (1), 13-9.
44. Fu, X. B.; Liu, D. D.; Lin, Y.; Hu, W.; Mao, Z. W.; Le, X. Y., Water-soluble DNA minor groove binders as potential chemotherapeutic agents: synthesis, characterization, DNA binding and cleavage, antioxidation, cytotoxicity and HSA interactions. *Dalton Trans.* **2014**, *43* (23), 8721-37.
45. (a) Baguley, B. C.; Denny, W. A.; Atwell, G. J.; Cain, B. F., Potential antitumor agents. 34. Quantitative relationships between DNA binding and molecular structure for 9-anilinoacridines substituted in the anilino ring. *J. Med. Chem.* **1981**, *24* (2), 170-7; (b) Matsuba, Y.; Edatsugi, H.; Mita, I.; Matsunaga, A.; Nakanishi, O., A novel synthetic DNA minor groove binder, MS-247: antitumor activity and cytotoxic mechanism. *Cancer Chemother. Pharmacol.* **2000**, *46* (1), 1-9.
46. Srivastava, M.; Nambiar, M.; Sharma, S.; Karki, S. S.; Goldsmith, G.; Hegde, M.; Kumar, S.; Pandey, M.; Singh, R. K.; Ray, P.; Natarajan, R.; Kelkar, M.; De, A.; Choudhary,

B.; Raghavan, S. C., An inhibitor of nonhomologous end-joining abrogates double-strand break repair and impedes cancer progression. *Cell* **2012**, *151* (7), 1474-87.

47. Yu, K.; Chedin, F.; Hsieh, C. L.; Wilson, T. E.; Lieber, M. R., R-loops at immunoglobulin class switch regions in the chromosomes of stimulated B cells. *Nat. Immunol.* **2003**, *4* (5), 442-51.

## Figure Legends

### Figure 1. Synthetic schemes of compounds MH1-5.

**Scheme-1. Synthesis of 2,5 disubstituted benzimidazole derivatives (MH1-2).** (a) Zn/HCl, EtOH, reflux; (b) T<sub>3</sub>P<sup>®</sup>, *p*-Tolualdehyde, Ethylacetate, 0°C-RT; (c) phenyl/4-bromo phenyl boronic acid, K<sub>2</sub>CO<sub>3</sub>, Bis(triphenylphosphine)palladium(II) dichloride, H<sub>2</sub>O:EtOH:1,4 dioxane (1:1:5), 130°C.

**Scheme-2. Synthesis of 2,5,7 trisubstituted benzimidazole derivatives (MH3-5) :** (i) Zn/HCl, EtOH, reflux; (ii) T<sub>3</sub>P<sup>®</sup>, *p*-Tolualdehyde/4-*tert*-Butylbenzaldehyde, Ethylacetate, 0°C-RT; (iii) phenyl/4-bromo phenyl boronic acid, K<sub>2</sub>CO<sub>3</sub>, Bis(triphenylphosphine)palladium(II) dichloride, H<sub>2</sub>O:EtOH:1,4 dioxane (1:1:5), 130°C.

**Figure 2. Chemical structure and yield of newly synthesized compounds.** Chemical structure of different benzimidazole derivatives and their respective yield is indicated.

**Figure 3. Cytotoxic effect of novel benzimidazole derivatives on different cancer cell lines.** Molt4, Nalm6, REH, MCF7, EAC, K562, and HeLa cells were treated with different concentrations (0-40 µM) of the compounds (**MH1**, **MH2**, **MH3**, **MH4** or **MH5**) for 48 or 72 h. MTT assay was performed for evaluating the effect of compounds on cell proliferation. **A)** IC<sub>50</sub> values for above compounds at 48 h as determined by MTT assay in different cancer cell lines. **B)** Bar diagram (mean ± SEM) showing effect of **MH1** (0, 1, 5, 10 and 20 µM) on proliferation of different leukemic cell lines (Molt4, Nalm6, K562 and REH respectively) at 48 and 72 h of treatment. Experiment was repeated a minimum of three times with good consensus.

**Figure 4. Cell cycle analysis of Molt4 and K562 cells following treatment with MH1.**

Molt4 and K562 cells were treated with different concentrations of **MH1** (0, 1, 5, 10 and 20  $\mu$ M for 48 h), fixed and analysed by flow cytometry after staining with propidium iodide. **A, C)** Histogram showing effect of **MH1** on Molt4 and K562 cells at 48 h. **B, D)** Bar diagram (n=2) showing percentage of cells in different cell cycle phases at 48 h of treatment with different concentrations of **MH1** on Molt4 and K562. **E, F)** Histogram showing effect of **MH1** (10  $\mu$ M) on cell cycle progression in Molt4 cells at different time points (3, 6, 12 and 24 h) and respective bar diagram showing cell cycle arrest (n=3).

**Figure 5. Evaluation of MH1 induced apoptosis by Annexin-FITC/PI staining.**

Molt4 cells treated with **MH1** (0, 1, 5 and 10  $\mu$ M for 48 h) were double-stained with Annexin-FITC/PI. **A)** Dot plots showing apoptotic cells following treatment with **MH1** on Molt4 cells. **B)** Bar diagram (n=2) representing distribution of early, late apoptotic and necrotic cell populations after treatment with **MH1**. **C)** Confocal images of Annexin-FITC/PI stained Molt4 cells, treated with **MH1** (0, 1, 5 and 10  $\mu$ M for 48 h).

**Figure 6. DNA fragmentation and live-dead cell assays following MH1 treatment in Molt4 cells.**

**A, B)** **MH1** treated (0, 1, 5 and 10  $\mu$ M for 48 h) Molt4 cells were stained with calcein-AM and ethidium homodimer and analysed by flow cytometry. Dot plot represents **MH1** treated Molt4 cells (A). Bar diagram (n=2) showing percentage of calcein-AM alone (live cells) or ethidium homodimer (dead cells) alone or calcein-AM/ ethidium homodimer stained Molt4 cells after treatment with **MH1**. **C and D)** Agarose gel stained with ethidium bromide showing DNA ladder formation in Molt4 cells after treatment with **MH1** (0, 1, 5, 10 and 20  $\mu$ M for 48 h). 'M' indicates DNA ladder and bar diagram representing quantification of HMW (high molecular weight) DNA and fragmented DNA.

**Figure 7. Evaluation of mitochondrial membrane potential and induction of apoptotic proteins in Molt4 cells following treatment with MH1.**

Molt4 cells were treated with different concentrations of **MH1** for 48 h and measured for mitochondrial membrane potential

by FACS and expression of apoptotic proteins by western blot analysis. **A)** Dot plot showing change in MMP following treatment with **MH1** (0, 1, 5, 10 and 20  $\mu\text{M}$ ). 2, 4-DNP treated Molt4 cells (48 h) served as positive control. **B)** Bar diagram (n=2) showing distribution of high, intermediate and low mitochondrial membrane potential in Molt4 cells after treatment with **MH1**. **C and D)** Immunoblotting showing differential expression/activation of apoptotic markers BAX, BCL2, CASPASE9, CASPASE3 following treatment with **MH1** in Molt4 cells (0, 1, 5 and 10  $\mu\text{M}$  at 48 h), actin served as the loading control and respective quantifications are given in terms of fold change.

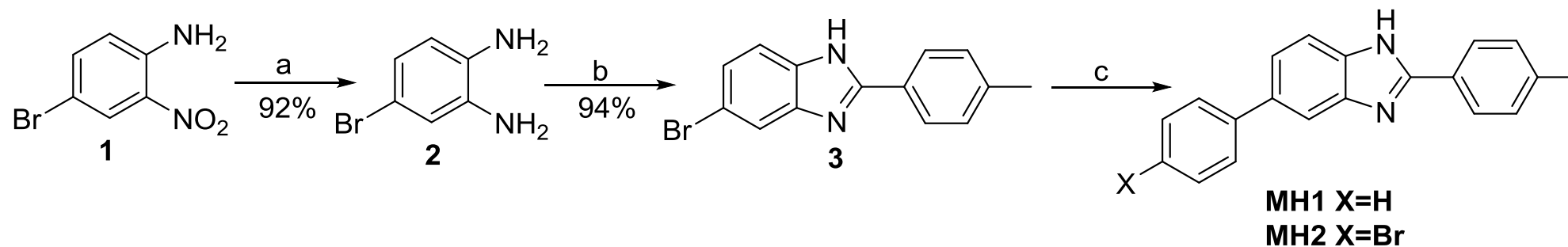
**Figure 8. Evaluation of MH1-DNA interaction by UV-visible, fluorescent spectroscopy and DNA dye displacement assays.** **A)** **MH1** was incubated with various concentrations of CT-DNA (0, 1, 5, 10, 25, 50, 75 and 100  $\mu\text{M}$ ) and absorbance was measured in UV-visible spectroscopy. The resulting spectra is shown as a function of wavelength. Arrow indicates increasing concentration of CT-DNA. **B)** Fluorescence emission spectra of **MH1** in presence of increasing concentrations of CT-DNA (0, 1, 5, 10, 25, 50, 75 and 100  $\mu\text{M}$ ). Arrow indicates increasing concentrations of CT-DNA. Fluorescence is expressed in RFU and is shown in Y-axis. **C)** Ethidium bromide dye displacement assay showing effect of increasing concentrations of **MH1** (0, 1, 5, 10, 25, 50 and 100  $\mu\text{M}$ ) on fluorescence emission spectra of ethidium bromide, when incubated with CT-DNA. Black spectral line indicates ethidium alone, red spectral line is ethidium bromide along with DNA and blue spectral lines are increasing concentrations of **MH1** and indicated by an arrow. **D)** Hoechst (33258) dye displacement assay showing effect of increasing concentrations of **MH1** (0, 1, 5, 10, 25, 50 and 100  $\mu\text{M}$ ) on fluorescence emission spectra of Hoechst along with CT-DNA. Yellow spectral line indicates Hoechst alone, red spectral line indicates Hoechst and CT-DNA, black spectral line is Hoechst with CT-DNA in presence of **MH3** (50  $\mu\text{M}$ ) and blue spectral lines indicate increasing concentrations of **MH1** and marked by an arrow.

**Figure 9. Evaluation of inhibitory effect of MH1 on topoisomerase action and transcription.** **MH1** inhibitory activity on human topoisomerase II $\alpha$  and T7 RNA polymerase

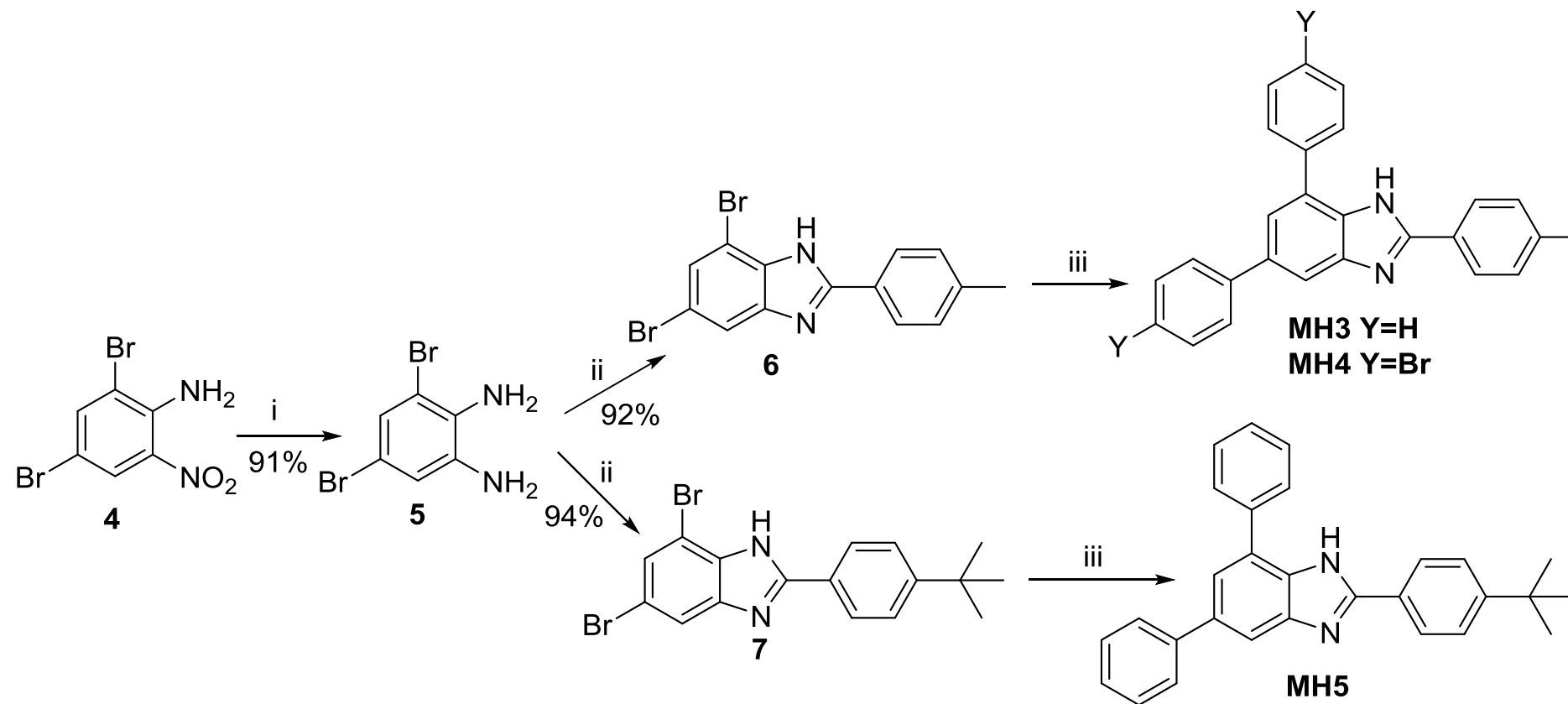


catalysed transcription was tested. **A)** Human topoisomerase II $\alpha$  activity was assayed in presence of increasing concentrations of **MH1** (0, 10, 25, 50 and 100  $\mu$ M) using supercoiled plasmid DNA (pBS-SK+, 37°C for 30 min). Etoposide (100  $\mu$ M) served as positive control, for the reaction. Supercoiled and relaxed forms of the DNA are indicated. **B)** Topoisomerase I assay in presence of **MH1**. Recombinant Human topoisomerase I was tested for its activity on supercoiled plasmid DNA in presence of different concentrations of **MH1** (0, 10, 25, 50 and 100  $\mu$ M) for 30 min at 37°C. Topotecan (7.5  $\mu$ M) was used as a positive control. Positions of supercoiled and relaxed DNA are indicated. **C)** *In vitro* transcription assay using T7 RNA polymerase was performed in presence of different concentrations of **MH1** (0, 10, 25, 50 and 100  $\mu$ M) for 30 min at 37°C. To confirm RNA species (denoted in red bracket) formation, products were also treated with RNase A (50  $\mu$ g/ml). 'M' is molecular weight ladder. **D)** Circular dichroism studies to check the topological changes in DNA in presence of **MH1**. CD analysis was carried out using CT-DNA (50  $\mu$ M) in presence of increasing concentrations of **MH1** (0, 10, 25, 50 and 100  $\mu$ M). Hoechst 33258 (10  $\mu$ M) was used as a positive control (black spectral line). DNA alone was presented in red spectral line.

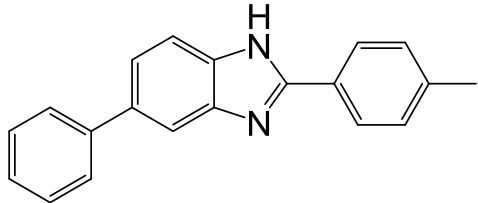
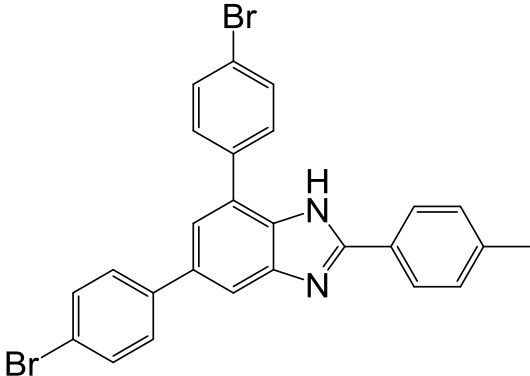
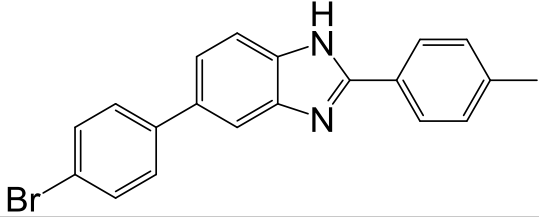
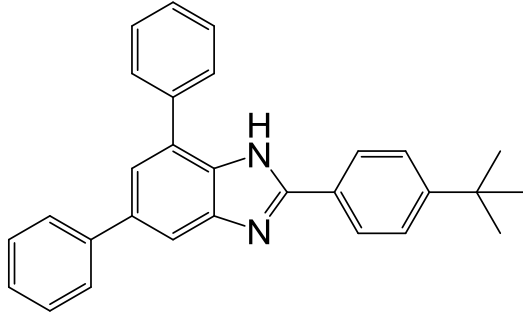
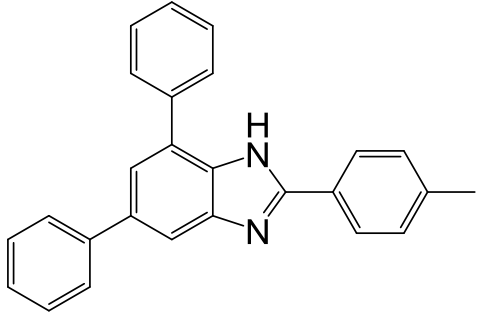
**Figure 10. Molecular docking studies of MH1 with double stranded DNA.** Ability of **MH1** to bind at the minor groove of DNA was tested with the help of Autodock 4.2 docking software and plausible interactions are represented. **A)** Docked orientation of **MH1** in Hoechst binding pocket of double stranded DNA (**MH1** is shown in cyan blue). **B)** Interaction of **MH1** at minor groove pocket of AT rich double-stranded DNA. **C)** Hydrogen bond formation between imidazole moiety of **MH1** and oxygen group of thymine residue inside the minor groove.



**Scheme-1. Synthesis of 2,5 disubstituted benzimidazole derivatives (MH1-2).** (a) Zn/HCl, EtOH, reflux; (b)  $T_3P^{\text{®}}$ , *p*-Tolualdehyde, Ethylacetate, 0<sup>0</sup>C-RT; (c) phenyl/4-bromo phenyl boronic acid,  $K_2CO_3$ , Bis(triphenylphosphine) palladium(II) dichloride,  $H_2O:EtOH:1,4$  dioxane (1:1:5), 130<sup>o</sup>C



**Scheme-2. Synthesis of 2,5,7 trisubstituted benzimidazole derivatives (MH3-5) :** (i) Zn/HCl, EtOH, reflux; (ii)  $T_3P^{\text{R}}$ , *p*-Tolualdehyde/4-*tert*-Butylbenzaldehyde, Ethylacetate, 0°C-RT; (iii) phenyl boronic acid/4-bromo phenyl boronic acid,  $K_2CO_3$ , Bis(triphenylphosphine)palladium(II) dichloride,  $H_2O:EtOH:1,4$  dioxane (1:1:5), 130°C.

Entry	Compound	Structure	Yield (%) <sup>a</sup>	Entry	Compound	Structure	Yield (%) <sup>a</sup>
1	MH1		84	4	MH4		75
2	MH2		78	5	MH5		81
3	MH3		82				

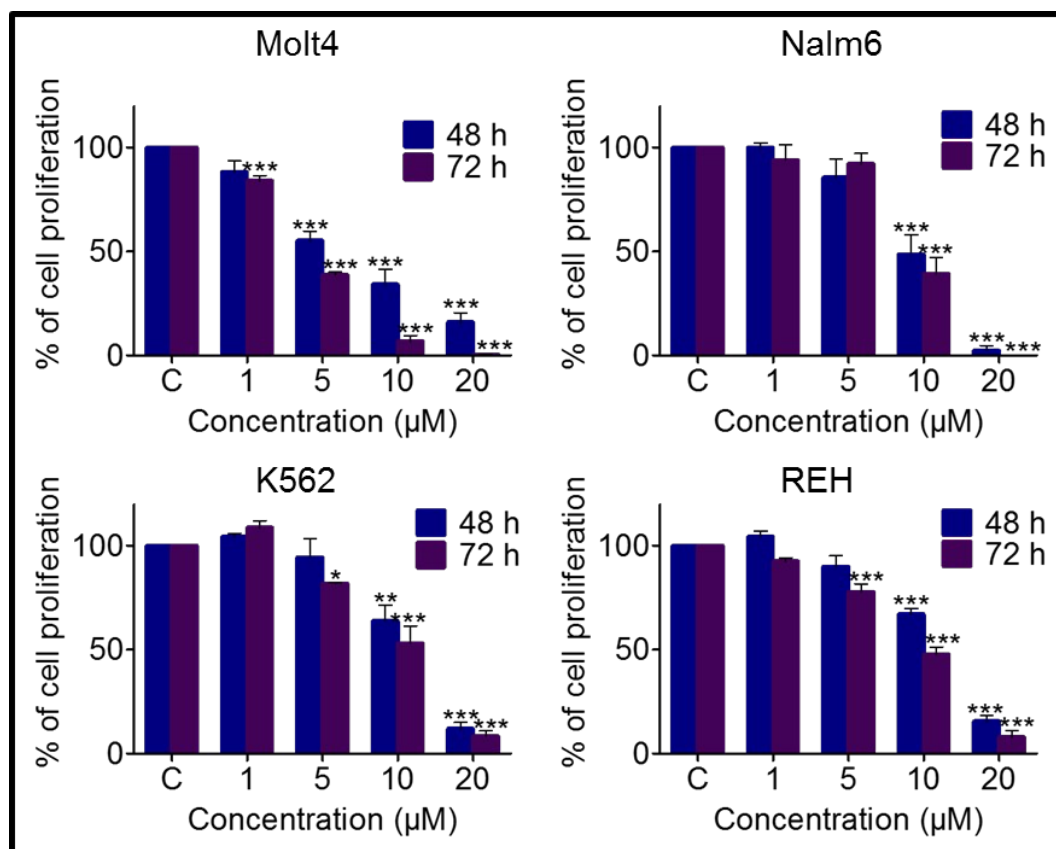
<sup>a</sup> Isolated yield based on intermediates **3, 6 & 7**

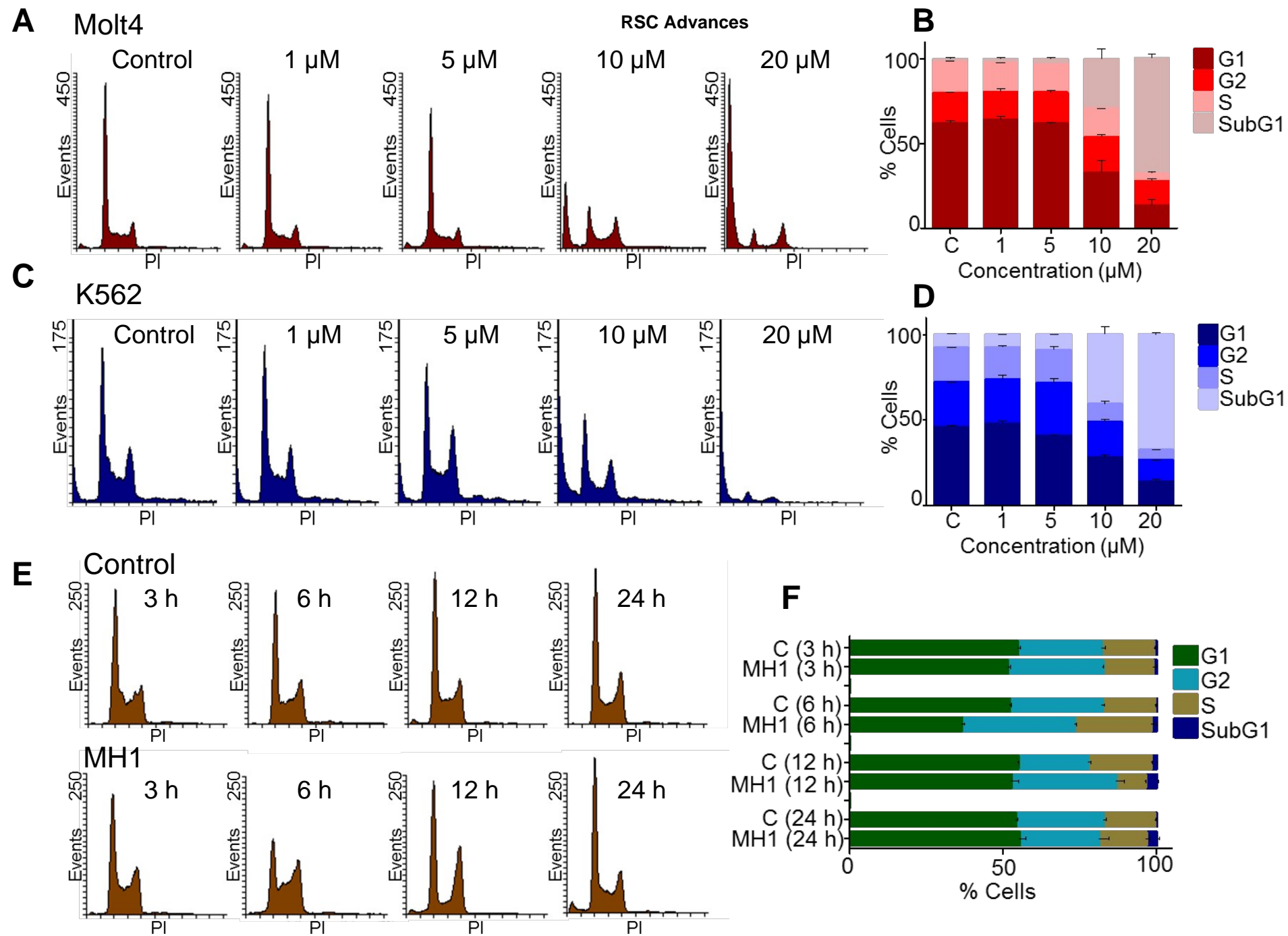
A

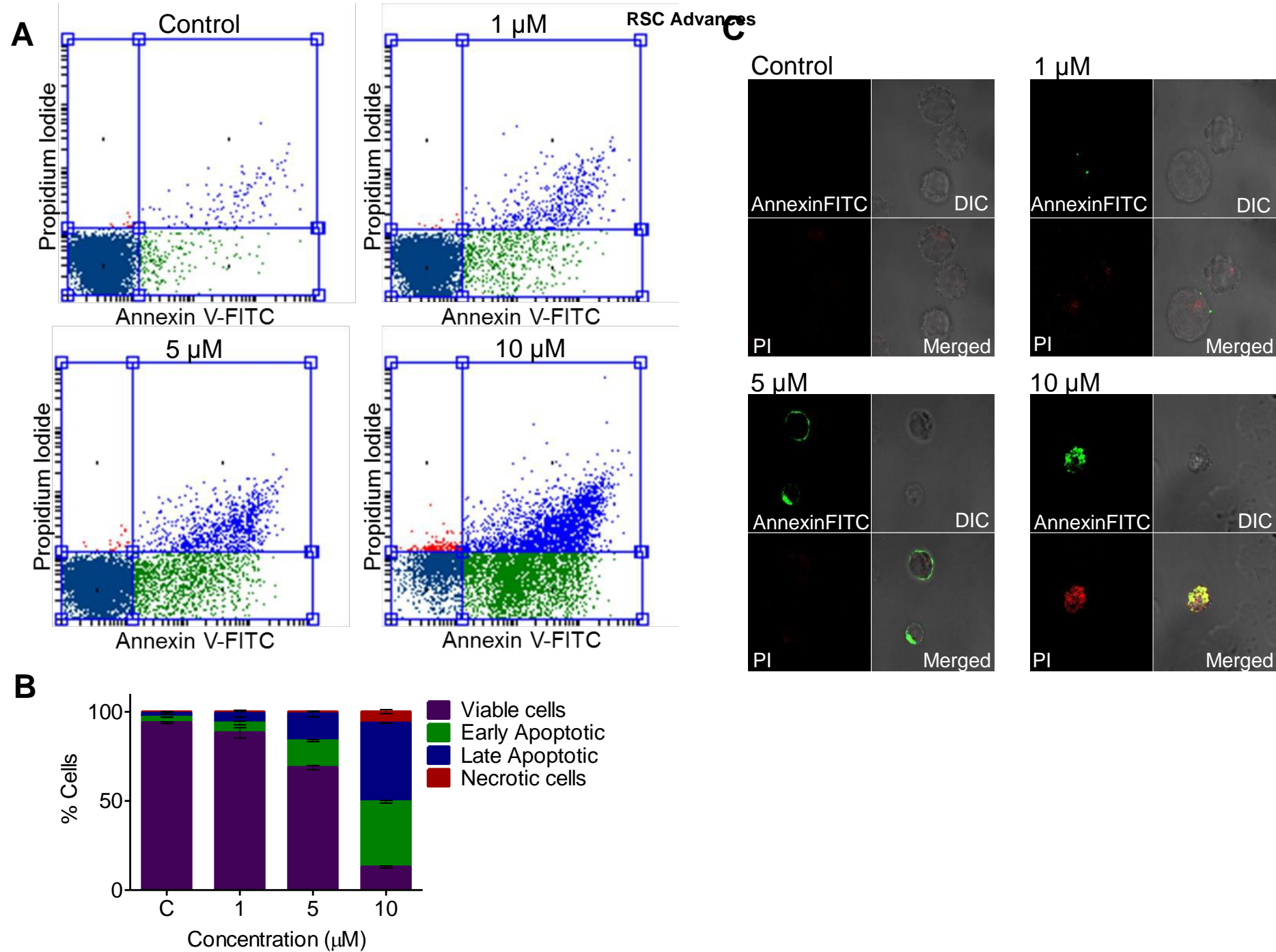
	Molt4	Nalm6	REH	MCF7	EAC	K562	HeLa
MH1	5.5 $\mu$ M	8.9 $\mu$ M	13.83 $\mu$ M	18.25 $\mu$ M	26.34 $\mu$ M	13.3 $\mu$ M	23.69 $\mu$ M
MH2	25.19 $\mu$ M	29.43 $\mu$ M	31.68 $\mu$ M	35.26 $\mu$ M	> 40 $\mu$ M	N.T	N.T
MH3	> 40 $\mu$ M	> 40 $\mu$ M	> 40 $\mu$ M	> 40 $\mu$ M	> 40 $\mu$ M	N.T	N.T
MH4	> 40 $\mu$ M	> 40 $\mu$ M	> 40 $\mu$ M	> 40 $\mu$ M	> 40 $\mu$ M	N.T	N.T
MH5	> 40 $\mu$ M	> 40 $\mu$ M	> 40 $\mu$ M	> 40 $\mu$ M	> 40 $\mu$ M	N.T	N.T

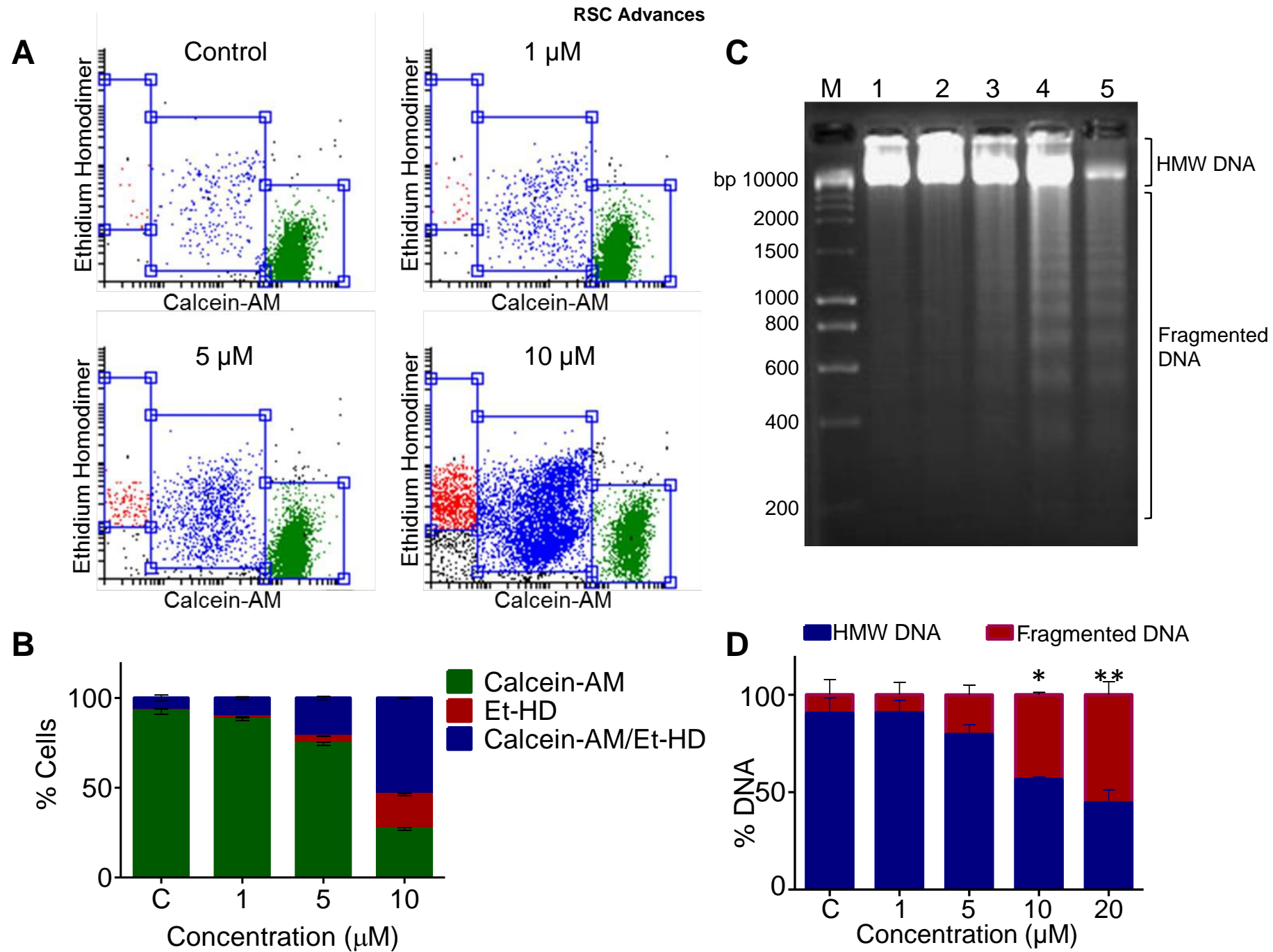
N.T- Not tested

B

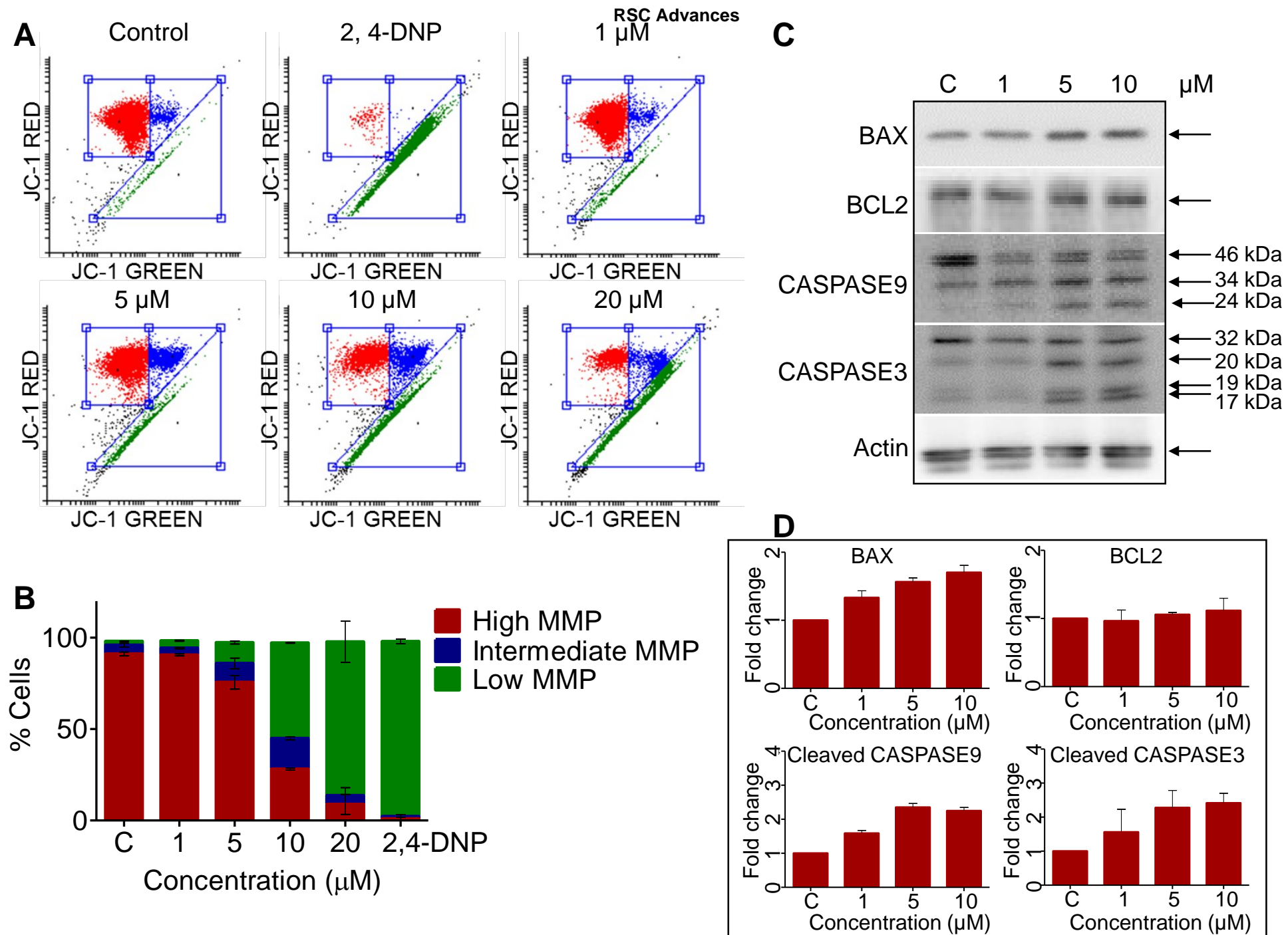












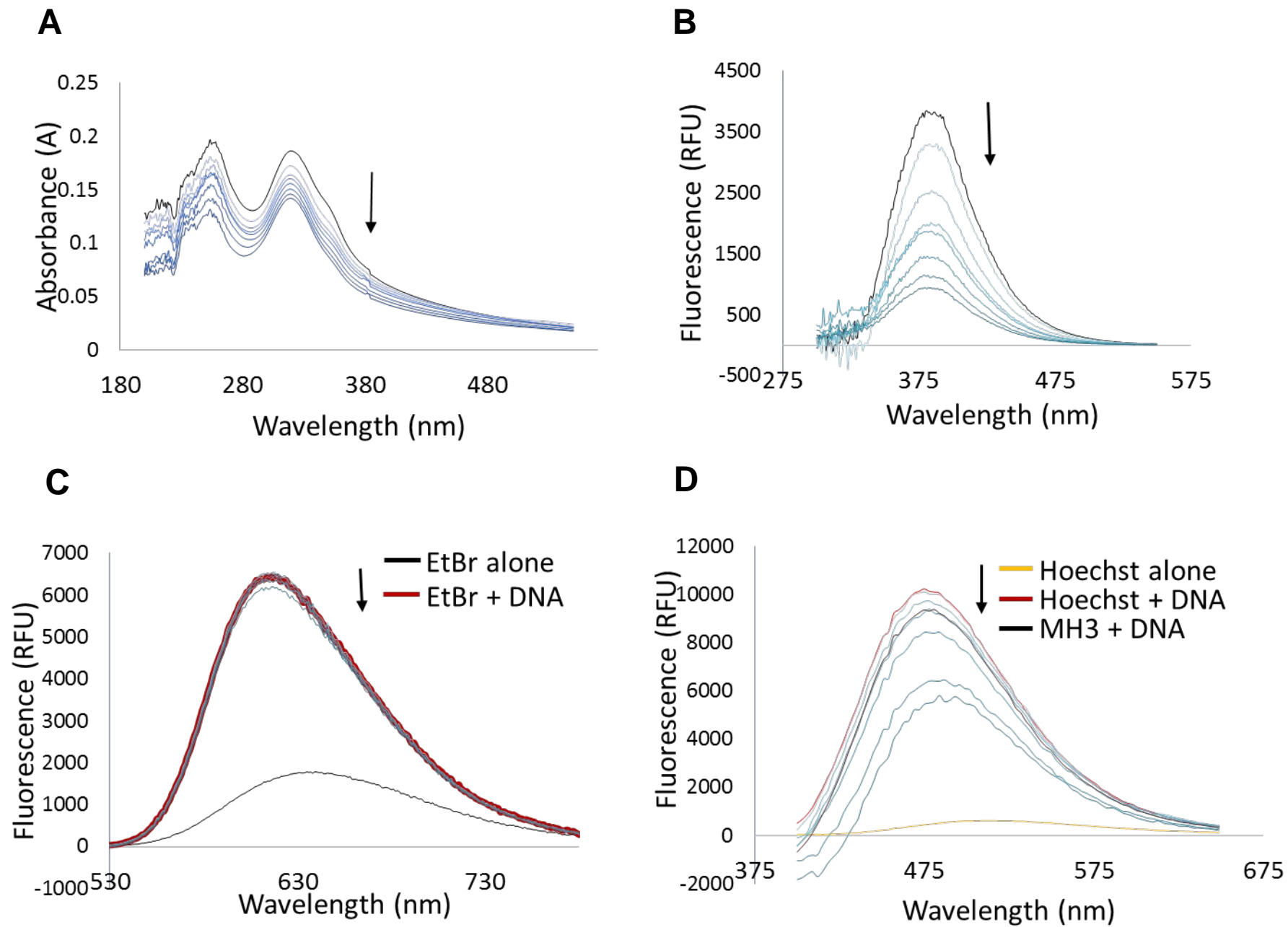
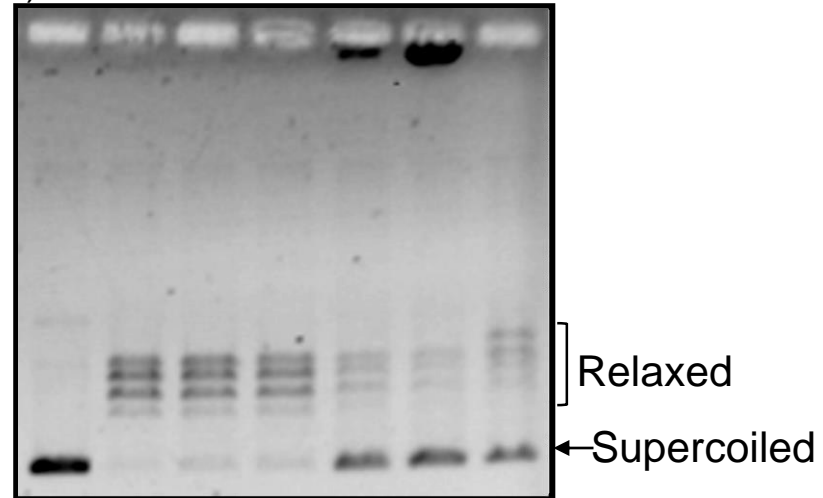


Figure 8

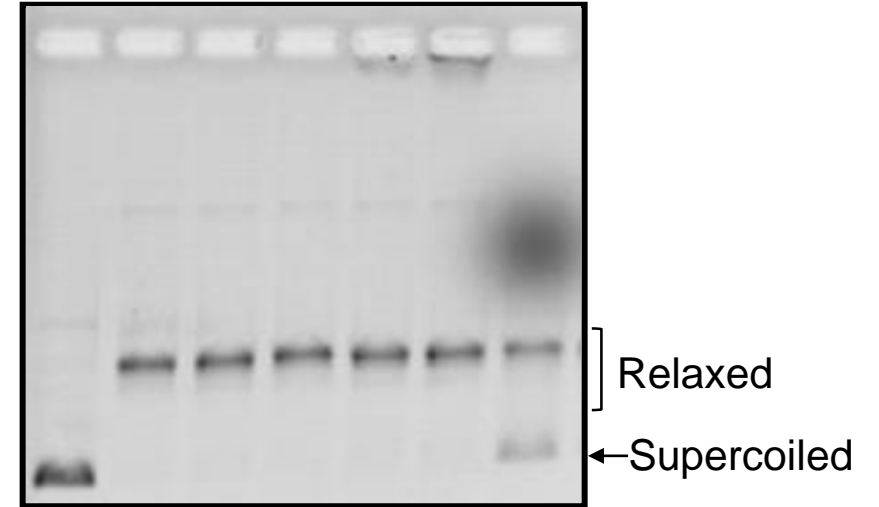
**A**

Topo II $\alpha$	-	+	+	+	+	+	+
MH1 ( $\mu$ M)	-	-	10	25	50	100	-
Etoposide ( $\mu$ M)	-	-	-	-	-	-	100



RSC Advance **B**

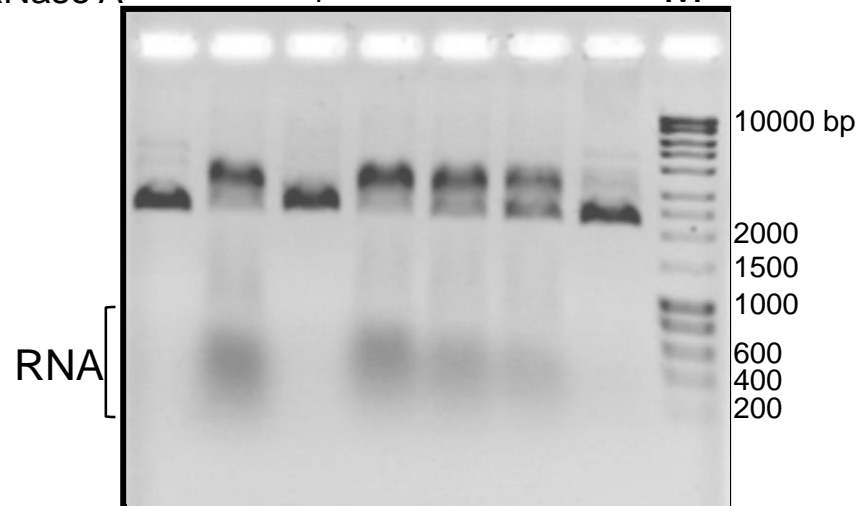
Topo I	-	+	+	+	+	+	+
MH1 ( $\mu$ M)	-	-	10	25	50	100	-
Topotecan ( $\mu$ M)	-	-	-	-	-	-	7.5



**C**

T7 RNA Pol	-	+	+	+	+	+	+
MH1 ( $\mu$ M)	-	-	-	10	25	50	100
RNase A	-	-	+	-	-	-	-

M



**D**

